Cell

Decoding the Signaling of a GPCR Heteromeric Complex Reveals a Unifying Mechanism of Action of Antipsychotic Drugs

Miguel Fribourg,[1,4] José L. Moreno,[2] Terrell Holloway,[2] Davide Provasi,[1] Lia Baki,[8] Rahul Mahajan,[8] Gyu Park,[8] Scott K. Adney,[8] Candice Hatcher,[8] José M. Eltit,[8] Jeffrey D. Ruta,[2] Laura Albizu,[3] Zheng Li,[1] Adrienne Umali,[2] Jihyun Shim,[7] Alexandre Fabiato,[8] Alexander D. MacKerell Jr.,[7] Vladimir Brezina,[1,4,6] Stuart C. Sealfon,[3,4,5,6] Marta Filizola,[1] Javier González-Maeso,[2,3,6,*] and Diomedes E. Logothetis[8,*]
[1]Department of Structural and Chemical Biology
[2]Department of Psychiatry
[3]Department of Neurology
[4]Department of Neuroscience
[5]Center for Translational Systems Biology
[6]Friedman Brain Institute
Mount Sinai School of Medicine, New York, NY 10029, USA
[7]Pharmaceutical Sciences Department, University of Maryland School of Pharmacy, Baltimore, MD 21201, USA
[8]Department of Physiology and Biophysics, Virginia Commonwealth University, School of Medicine, Richmond, VA 23298, USA
*Correspondence: javier.maeso@mssm.edu (J.G.-M.), delogothetis@vcu.edu (D.E.L.)
DOI 10.1016/j.cell.2011.09.055

SUMMARY

Atypical antipsychotic drugs, such as clozapine and risperidone, have a high affinity for the serotonin 5-HT_{2A} G protein-coupled receptor (GPCR), the 2AR, which signals via a G_q heterotrimeric G protein. The closely related non-antipsychotic drugs, such as ritanserin and methysergide, also block 2AR function, but they lack comparable neuropsychological effects. Why some but not all 2AR inhibitors exhibit antipsychotic properties remains unresolved. We now show that a heteromeric complex between the 2AR and the G_i-linked GPCR, metabotropic glutamate 2 receptor (mGluR2), integrates ligand input, modulating signaling output and behavioral changes. Serotonergic and glutamatergic drugs bind the mGluR2/2AR heterocomplex, which then balances Gi- and Gq-dependent signaling. We find that the mGluR2/2AR-mediated changes in Gi and Gq activity predict the psychoactive behavioral effects of a variety of pharmacological compounds. These observations provide mechanistic insight into antipsychotic action that may advance therapeutic strategies for disorders including schizophrenia and dementia.

INTRODUCTION

G protein-coupled receptors (GPCRs) are the most common cellular targets for drugs used in the clinic (Rosenbaum et al., 2009). Agonist binding is thought to induce distinct conformational changes that enable GPCRs to couple to and activate specific heterotrimeric G proteins (Oldham and Hamm, 2008). For example, 2AR is a Gq-coupled GPCR that responds to the neurotransmitter serotonin (5-HT) (González-Maeso and Sealfon, 2009), and mGluR2 is a Gi-coupled, pertussis toxin-sensitive GPCR that responds to the neurotransmitter glutamate (Glu) (Moreno et al., 2009). Although considerable biochemical and biophysical data are consistent with monomeric GPCRs binding and activating G proteins (Ernst et al., 2007; Whorton et al., 2007), several recent studies suggest that G protein coupling in cell membranes involves the formation of homomeric and heteromeric GPCR complexes (Han et al., 2009; Lopez-Gimenez et al., 2007; Carriba et al., 2008; Vilardaga et al., 2008). Oligomeric receptor complexes appear to exhibit distinct signaling properties when compared to monomeric receptors (Urizar et al., 2011; Milligan, 2009). The molecular mechanism(s) responsible for such changes in pharmacology are poorly understood, as is the physiological function of GPCR heteromeric complexes.

Atypical antipsychotic drugs have a high affinity for the 2AR (Meltzer et al., 1989; Meltzer and Huang, 2008) and are widely used in the treatment of schizophrenia and other psychiatric disorders (Ross et al., 2006). Interestingly, it has been recently recognized that most clinically effective antipsychotic drugs are, in fact, 2AR inverse agonists—ligands that preferentially bind and stabilize a GPCR in an inactive conformational state (Kenakin, 2002)—rather than simply neutral antagonists (Aloyo et al., 2009; Egan et al., 1998; Weiner et al., 2001)—ligands that compete for the same orthosteric binding site and prevent the cellular responses induced by agonists and inverse agonists. The mechanism underlying the antipsychotic effects of 2AR inverse agonism has not yet been elucidated.

A new class of potential antipsychotic drugs acting as agonists of mGluR2 recently received attention in preclinical (Woolley

et al., 2008) and clinical studies (Patil et al., 2007, Kinon et al., 2011). Previous work demonstrated that mGluR2 and 2AR form a specific heterocomplex in mammalian brain tissue (González-Maeso et al., 2008; Rives et al., 2009). However, the signaling properties of this receptor heterocomplex and its role in transducing antipsychotic drug activity remain unclear. Here, we compare G protein signaling coupled to the heteromeric mGluR2/2AR complex with homomeric signaling through either mGluR2 or 2AR. Our results provide insight into how Gi and Gq signaling are integrated by this GPCR heteromer and uncover a unifying mechanism of action of two families of antipsychotic drugs that target the mGluR2/2AR heteromeric complex. In addition, we provide a predictive metric for the anti- or propsychotic effects of serotonergic and glutamatergic ligands.

RESULTS

Heteromeric Assembly of mGluR2 and 2AR Enhances Glutamate-Elicited Gi Signaling and Reduces 5-HT-Elicited Gq Signaling

2AR and mGluR2 proteins colocalize in mouse cortical slices and neuronal primary cultures (Figure 1A and Figure S1E available online). In addition, the two receptors can be coimmunoprecipitated from mouse frontal cortex (Figure 1B). To investigate the signaling properties of the mGluR2/2AR heterocomplex, we utilized a *Xenopus* oocyte heterologous expression system (Barela et al., 2006). We expressed each of these GPCRs alone or together and used inhibition of the IRK3 (Kir2.3) current to monitor 2AR-elicited Gq activity (Figure 1C, left) (Du et al., 2004) and activation of the GIRK4* (or Kir3.4*) current to monitor mGluR2-elicited Gi activity (Figure 1C, right) (He et al., 1999, 2002) (see Experimental Procedures).

How do the signaling properties of the mGluR2/2AR heteromeric complex differ from those of the homomeric receptors? We first quantified the Gi and Gq activities evoked by Glu and 5-HT, the endogenous ligands of the mGluR2 and 2AR receptors, respectively, and compared these values to Gi and Gq activities in the absence or presence of the heteromeric receptor partner (Figures 1C–1E). Coexpression of mGluR2 with the 2AR reduced 5-HT-elicited Gq activity by approximately 50% (Figures 1C, left panel and 1D). In contrast, coexpression of mGluR2 with the 2AR increased the Glu-elicited Gi activity by nearly 200% (Figure 1C, right panel and 1E).

The metabotropic glutamate receptor 3 (mGluR3), which shares a high degree of homology with mGluR2, does not form a receptor heterocomplex with the 2AR. Exchanging the transmembrane (TM) domains of mGluR2 and mGluR3 either disrupts (mGluR2Δ) or rescues (mGluR3Δ) mGluR2/2AR receptor complex formation and 2AR-mediated cross-signaling (i.e., Gi signaling) (González-Maeso et al., 2008). mGluR2Δ activation does not evoke the Gi and Gq signaling outputs associated with the mGluR2/2AR heteromer, whereas mGluR3Δ activation induces an increase in Gi- and decrease in Gq-dependent signaling (Figures S1A–S1D). Each of the mGluR chimeras, when expressed as homomers, showed intact Gi signaling (Figures S2A–S2C) and cell-surface localization (Figure S2D). Together these findings suggest that the heteromeric receptor couples Gi and Gq outputs to influence downstream signaling events.

To summarize the difference between Gi and Gq signaling evoked by the mGluR2/2AR heteromers, we developed a metric called the balance index (BI). The BI combines the change in Gi activity (ΔGi) and the change in Gq activity (ΔGq), such that BI = ΔGi − ΔGq (Figure 1F). We used homomeric Gi and Gq signaling levels to normalize the data and found that without stimulation, the mGluR2/2AR complex yielded a BI of 1.45, which we use as the reference BI level (BI_r). We obtained the largest BI_r when expressing mGluR2/2AR mRNAs in a 1:2 ratio (Figure S3D). As shown in Figure S3C, this ratio of mRNAs yielded a cell-surface localization of receptor protein levels that suggested a higher-order oligomeric complex between mGluR2 and 2AR (see Figures S3A and S3B).

Drugs that Bind 2AR Alter the Balance between Gi and Gq Signaling

We next asked whether drugs bound to one receptor of the heteromer could affect the other receptor's signaling response to its endogenous ligand. We first investigated the effects of 2AR ligands (a neutral antagonist, a strong agonist, and an inverse agonist) on Glu-elicited Gi signaling by mGluR2. We define DOI as a strong agonist because it evokes greater Gq signaling through 2AR than the endogenous ligand, 5-HT (Figures 2A, 2B, and S4A). In control experiments, the strong agonist (DOI), the neutral antagonist (methysergide), and the inverse agonist (clozapine) (Weiner et al., 2001) worked as expected to stimulate or reduce 5-HT-induced Gq signaling, respectively (Figure 2A).

Occupancy of the 2AR by either methysergide, DOI, or clozapine had different effects on Glu-elicited signaling through mGluR2 (Figure 2B, blue bars). Although Glu-elicited Gi signaling was not altered by 5-HT or methysergide, it was decreased back to baseline by DOI and increased by approximately 40% (240% greater than homomeric levels) by clozapine (Figure 2B).

Using the results obtained for Gi (Figure 2B, blue bars) and Gq signaling (Figures 2A and 2B, red bars), we calculated the BI values for the three ligands in the presence of the endogenous ligands (Figure 2C). The changes evoked by these three drugs were abrogated by mGluR2Δ or mimicked by mGluR3Δ (see Table S1), and they were present when the Gq pathway was blocked by the regulator of G protein signaling subunit 2 (RGS2) (Figures S5D and S5E). The 2AR ligand with the largest overall BI was the inverse agonist clozapine (BI = 2.30; 140% increase in Gi and 100% decrease in Gq).

Could these ligands exert their effects by stabilizing different conformations of the receptor complex? To address this question, we investigated the conformational changes induced by the three 2AR ligands in molecular models of 2AR alone or complexed with mGluR2. To observe large conformational changes in relatively short timescales, we used a combination of adiabatic-biased molecular dynamics (ABMD) and metadynamics simulations (see "Computational Methods" in Experimental Procedures). This approach was recently validated on a prototypic GPCR (Provasi et al., 2011). First, we studied the effects of methysergide, DOI, and clozapine on the activation free-energy profile of a protomeric 2AR (see Figure 2D, top) and identified the most energetically favorable 2AR state for each ligand.

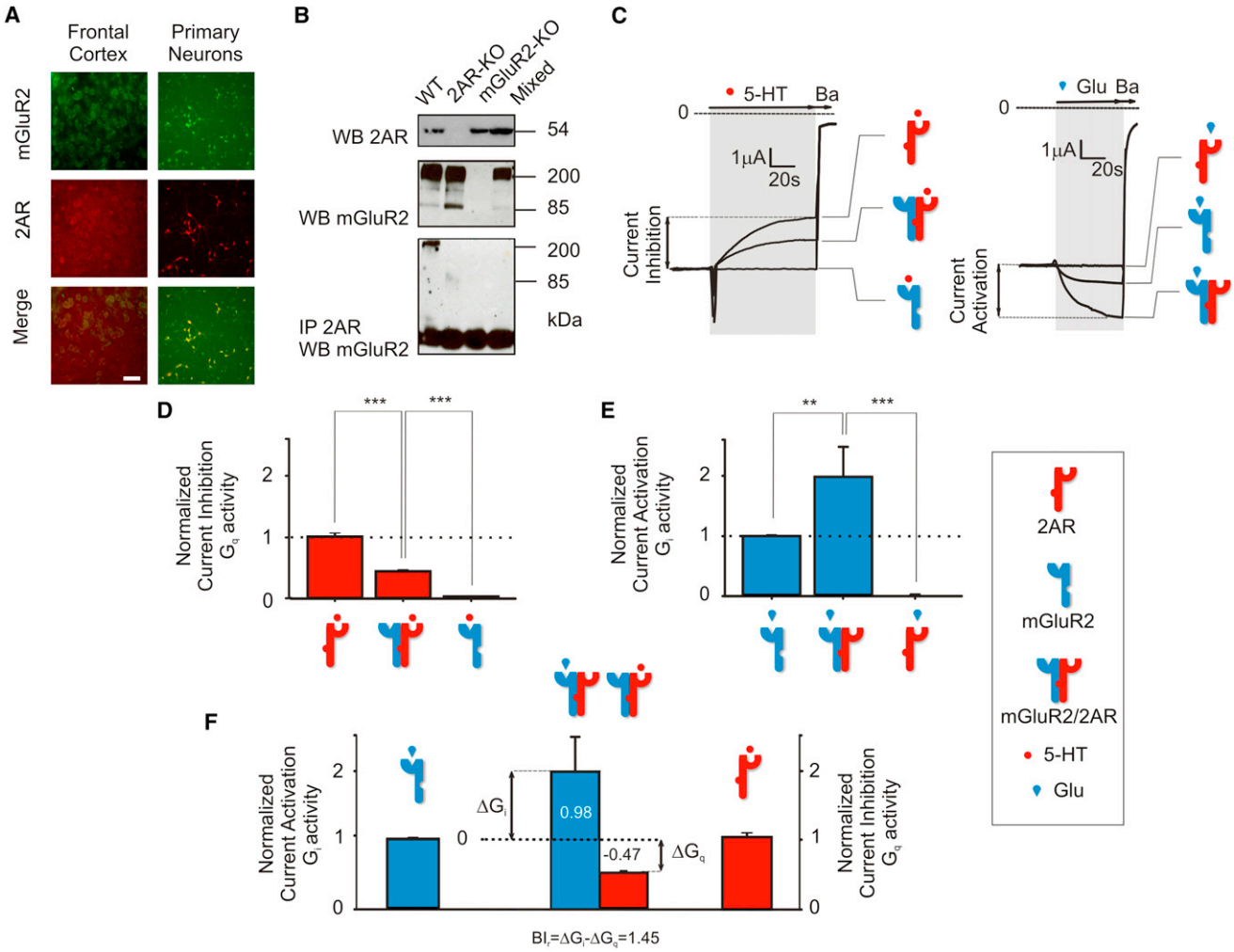

Figure 1. Heteromeric Assembly of 2AR and mGluR2 Enhances Glu-Induced Gi Signaling and Reduces 5-HT-Induced Gq Signaling

(A) Representative micrographs showing coexpression of endogenous 2AR (red) and mGluR2 (green) in mouse frontal cortex (left panels) and mouse cortical primary neurons (right panels). Scale bar, 25 μm. See also Figure S1E. 2AR and mGlu2 colocalize and form a receptor complex in mouse frontal cortex.

(B) Mouse frontal cortex membrane preparations were immunoprecipitated (IP) with anti-2AR antibody. Immunoprecipitates were analyzed by western blot (WB) with anti-mGluR2 antibody (lower blot). Mouse frontal cortex membrane preparations were also directly analyzed by WB with anti-2AR antibody (upper blot) or anti-mGluR2 antibody (middle blot). 2AR-KO and mGluR2-KO mouse frontal cortex tissue samples were processed identically and used as negative controls. Frontal cortex tissue samples from 2AR-KO and mGluR2-KO mice were also homogenized together (mixed) and processed identically for immunoprecipitation and WB.

(C) Representative barium-sensitive traces of IRK3 currents obtained in response to 1 μM 5-HT in oocytes expressing 2AR alone, mGluR2 and 2AR together, or mGluR2 alone (left). Representative barium-sensitive traces of GIRK4* currents obtained in response to 1 μM Glu in oocytes expressing mGluR2 alone, mGluR2 and 2AR together, or 2AR alone (right). Barium (Ba) inhibited IRK3 and GIRK4* currents and allowed for subtraction of IRK3- and GIRK4*-independent currents. For illustrative purposes, traces with similar basal currents were chosen.

Summary bar graphs of (D) Gq activity measured as IRK3 current inhibition (mean ± standard error of the mean [SEM]) following stimulation with 5-HT and (E) Gi activity measured as GIRK4* current activation (mean ± SEM) following stimulation with Glu. IRK3 current inhibition was measured relative to basal currents and was normalized relative to that obtained by stimulating 2AR alone with 5-HT (100% or 1). GIRK4* current activation was measured relative to the basal currents and was normalized relative to that obtained by stimulating mGluR2 alone with Glu (100% or 1).

(F) Calculation of the BI as the difference of the increase in Gi signaling in response to Glu from the mGluR2 homomeric level (ΔGi) and the decrease of Gq signaling in response to 5-HT from the 2AR homomeric level (ΔGq). A reference BI (Bi_r = 1.45) was calculated for the mGluR2/2AR complex in response to 1 μM Glu and 1 μM 5-HT using mean values (**p < 0.01, ***p < 0.001). Error bars depict standard error of the mean (SEM).

See also Figures S1, S2, and S3.

In agreement with known efficacies of these ligands, the clozapine-bound 2AR conformation is inactive (i.e., 2RH1-like), the DOI-bound 2AR conformation is active (i.e., 3P0G-like), and the methysergide-bound conformation adopts an inactive state that is structurally different from the inactive state stabilized by clozapine.

To provide a structural context for the crosstalk between 2AR and mGluR2, we studied the effects of the three 2AR

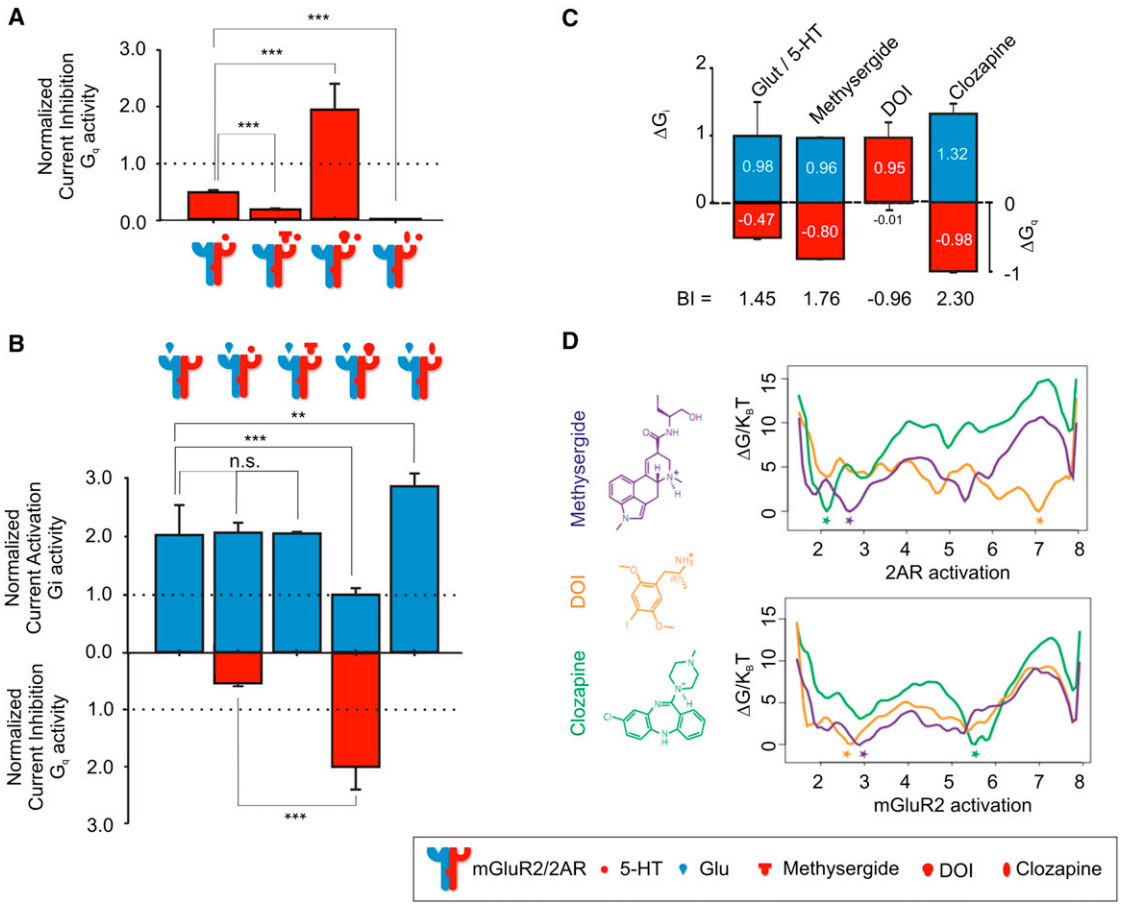

Figure 2. Drugs that Target 2AR: Integrative Effects on Gi and Gq Signaling

(A) Summary bar graphs of Gi activity (mean ± SEM) measured in oocytes expressing mGluR2/2AR following stimulation with 1 μM 5-HT alone or together with 10 μM methysergide, 10 μM DOI, or 10 μM clozapine. Gq activity was normalized relative to that obtained by stimulation of 2AR alone with 5-HT (100% or 1, dotted line).

(B) Summary bar graphs of Gi activity (top) and Gq activity (bottom) (mean ± SEM) measured in oocytes expressing mGluR2/2AR following stimulation with 1 μM Glu alone or together with 10 μM methysergide, 10 μM DOI, or 10 μM clozapine. Gi and Gq activity was normalized relative to the response to Glu and 5-HT, respectively (100% or 1, dotted line).

(C) ΔGi referenced to the homomeric mGluR2 response to 1 μM Glu and ΔGq referenced to the homomeric 2AR response to 1 μM 5-HT together with 10 μM methysergide, 10 μM DOI, or 10 μM clozapine (**$p < 0.01$, ***$p < 0.01$, n.s.: not significant). Data are mean ± SEM.

(D) Metadynamics-based mechanistic interpretation of functional crosstalk between 2AR and mGluR2. (Top) Activation profile of 2AR in the presence of different ligands. Free energy of the 2AR bound to the inverse agonist clozapine (green), the neutral antagonist methysergide (purple), and the dominant agonist DOI (orange), as a function of the position along the path connecting the inactive (s = 1) to the active (s = 8) states, is shown. (Bottom) Activation profile of mGluR2 in the presence of the different ligand-specific 2AR conformations. The three lines correspond to the activation free-energy profile of mGluR2 in dimeric complex through a TM4-TM4 interface with 2AR bound to the inverse agonist clozapine (green line), a TM4,5-TM4,5 interface with 2AR bound to the neutral antagonist methysergide (purple), and a TM4,5-TM4,5 interface with 2AR bound to the dominant agonist DOI (orange line). The most energetically stable states are indicated by a star, and the chemical structures of the three drugs are also shown.

ligands on mGluR2 conformations in the dimeric complex. Figure 2D (bottom) shows that when clozapine is bound to 2AR, the mGluR2 equilibrium shifts toward an activated conformation (i.e., 3DBQ-like), consistent with functional upmodulation of Gi signaling. In contrast, when methysergide and DOI are bound to 2AR, mGluR2 is stabilized in inactive states (i.e., 1U19-like). Although no significant energetic and structural differences were noted between the TM regions of these inactive states, the functional downmodulation of Gi signaling induced by DOI, but not by methysergide, may be ascribed to different interactions between the receptor loop regions and the G protein, which are not taken into account in our simulations. The functional predictions from this computational approach can be used to guide structure-based rational discovery of novel "biased" drugs that are capable of selectively activating specific signaling pathways.

Together, these results indicate that formation of the heteromer enables modulation of the mGluR2-Gi response by 2AR ligands. Whereas drugs such as the strong 2AR agonist DOI can greatly stimulate Gq signaling and decrease Gi signaling (henceforth referred to as dominant agonists), inverse agonists, such as clozapine, have the opposite effect, abolishing Gq and increasing Gi signaling.

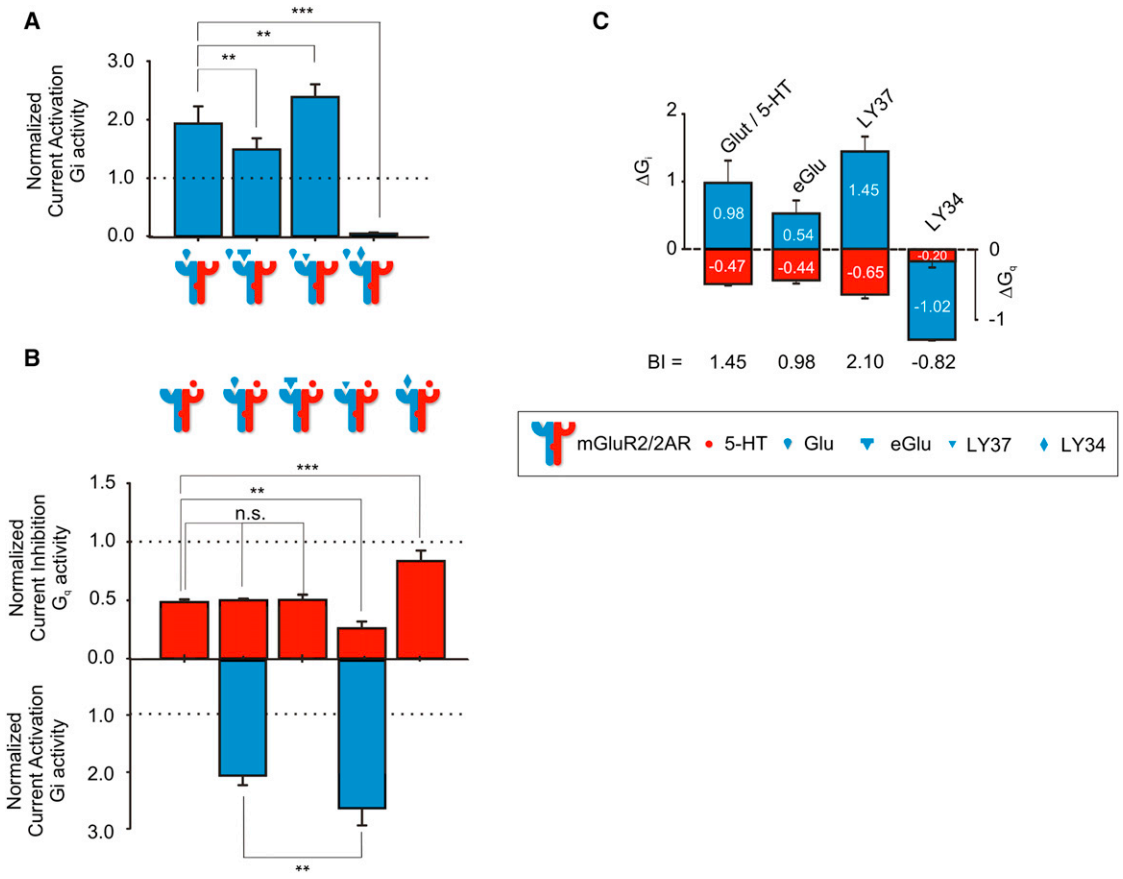

Figure 3. Drugs that Target mGluR2: Integrative Effects on Gi and Gq Signaling

(A) Summary bar graphs of Gi activity (mean ± SEM) measured in oocytes expressing mGluR2/2AR following stimulation with 1 μM Glu alone or together with 10 μM eGlu, 10 μM LY37, or 10 μM LY34. Gi activity was normalized relative to that obtained by stimulation of mGluR2 alone with 5-HT (100% or 1, dotted line).

(B) Summary bar graphs of Gq activity (red) and Gi activity (blue) (mean ± SEM) measured in oocytes expressing mGluR2/2AR following stimulation with 1 μM 5-HT alone or together with 10 μM eGlu, 10 μM LY37, or 10 μM LY34. Gq and Gi activities were normalized relative to the response to 5-HT and Glu, respectively (100% or 1, dotted line).

(C) ΔGi referenced to the homomeric mGluR2 response to 1 μM Glu and ΔGq referenced to the homomeric 2AR response to 1 μM 5-HT together with 10 μM methysergide, 10 μM DOI, or 10 μM clozapine (**$p < 0.01$, ***$p < 0.01$, n.s.: not significant). Data are mean ± SEM.

See also Figures S4 and S5.

Drugs that Bind mGluR2 Alter the Balance between Gi and Gq Signaling

How do drugs bound to the mGluR2 component of the heteromer affect the 5-HT-elicited Gq signaling of the 2AR? Neutral antagonist ethylglutamic acid (eGlu), the strong agonist (LY37) (Figure S4B), and the inverse agonist (LY34) (Figure S4C) worked as expected to reduce, stimulate, or abolish Glu-elicited Gi signaling through mGluR2, respectively (Figure 3A). Consistent with its inverse-agonist properties, LY34 not only completely abolished Gi signaling but also reduced the basal Gi activity of the mGluR2 receptor even in the absence of Glu (Figure S4C).

Occupancy of the mGluR2 receptor by each of the three ligands influenced the 2AR signaling. Relative to the homomeric 2AR levels, formation of the complex reduced the extent of Gq signaling by 50% (Figures 3B, 1D, and 1F). Although 5-HT-elicited Gq signaling was unaffected by Glu or eGlu, it was further decreased by LY37 and restored to near-homomeric levels by LY34 (Figure 3B).

Using the data shown for Gi (Figures 3A and 3B, blue bars) and Gq signaling (Figure 3B, red bars), we calculated the BI values for the three ligands (Figure 3C). As with 2AR drugs, the neutral antagonist eGlu only affected the mGluR2 side of signaling. The strong agonist LY37, however, affected both types of signaling through the complex and showed a dominant-agonist behavior as defined previously. Furthermore, LY37, like DOI, cross-signaled and elicited Gq signaling in the absence of Glu and 5-HT, respectively (Figures S4F and S4G). The inverse agonist LY34 had the opposite two effects: it blocked Gi but also potentiated Gq signaling, achieving almost 2AR homomeric levels (83%). All effects were disrupted when replacing mGluR2 by mGluR2Δ or rescued by mGluR3Δ (see Table S1), and they were present when the Gi pathway was blocked by pertussis toxin (PTX) (Figures S5A–S5C). The largest overall signaling difference between Gi and Gq was obtained by the dominant agonist LY37 (BI = 2.10).

In summary, the formation of the heteromeric complex favors Gi over Gq signaling by endogenous ligands. Dominant agonists

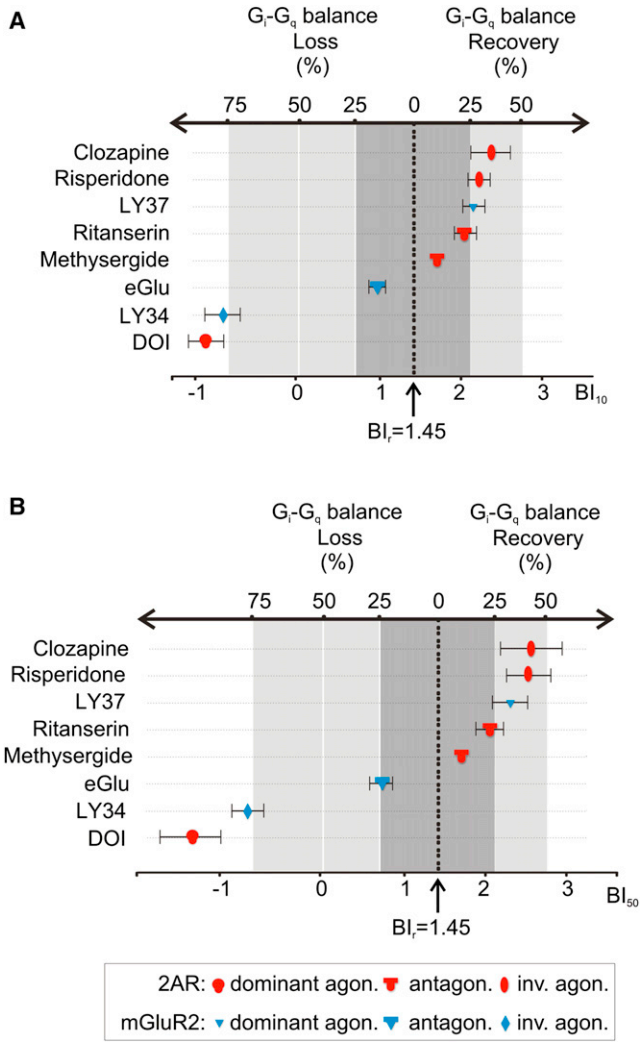

Figure 4. Use of BI to Classify Anti-/Propsychotic Propensity of Drugs Targeting the mGluR2/2AR Complex

Correlation maps between the BI and percentage of Gi-Gq balance loss or recovery for different drugs assuming a fractional occupancy of the heteromer by the drug of 0.5 (see Experimental Procedures). BIs were calculated for 10 μM (BI_{10}) (A) and 50 μM (BI_{50}) (B) concentrations of the drugs together with 1 μM Glu and 1 μM 5-HT and placed accordingly in the horizontal axis. BI_r = 1.45 corresponds to zero. Effects on the difference between Gi and Gq signaling are shown for drugs with known antipsychotic effects like clozapine, risperidone, and LY37, for ritanserin, an antidepressant, for neutral antagonists methysergide and eGlu, for the psychedelic DOI, and for the propsychotic LY34 (see also Table S1). Error bars depict SEM.

enhance signaling through the receptor they target as part of the complex but inhibit signaling of the heteromeric receptor partner. Inverse agonists inhibit signaling through the receptor they target as part of the complex but enhance signaling of the heteromeric receptor partner.

The BI Predicts the Anti- or Propsychotic Activity of Drugs Targeting mGluR2 or 2AR

Our results in Figures 2 and 3 indicate that although clozapine and LY37 act on different receptors, both drugs act through the mGluR2/2AR complex to achieve a similar effect—an increase in Gi activity with a concomitant decrease in Gq activity. To test whether the psychoactive effects of specific drugs correlated with differences in the levels of Gi and Gq activity that they induced, we calculated BI values for multiple drugs. For mGluR2, in addition to the dominant agonist LY37, we tested the neutral antagonist eGlu and the inverse agonist LY34, a drug that has been shown to increase locomotor activity and exploratory behavior in mice and might be propsychotic (Bespalov et al., 2007). For 2AR, besides the inverse agonist clozapine, we tested the following: risperidone, another widely used atypical antipsychotic like clozapine; ritanserin, an antidepressant also used as an adjuvant therapeutic for schizophrenia; methysergide, a neutral antagonist mainly used for migraines; and DOI, a propsychotic drug with lysergic acid diethylamide (LSD)-like effects.

In the presence of endogenous ligands and absence of drugs, the difference between Gi and Gq signaling is naturally kept in a balance that favors Gi over Gq (BI_r). We set the reference level of the BI scale to BI_r = 1.45 and compared the relative effect of different drugs on the BI, assuming a 50% occupancy of the receptor by the drug (see Gi-Gq recovery/loss calculation in Experimental Procedures). Results from drugs that target mGluR2 (blue icons), versus those that target 2AR (red icons), are plotted in Figure 4.

Drugs with the most effective antipsychotic properties, regardless of the receptor they target (2AR: clozapine, risperidone; mGluR2: LY37), show the highest BI values. In contrast, drugs with the most effective propsychotic properties (2AR: DOI; mGluR2: LY34) show the lowest BI values (Figure 4 and Table S2). All of these drugs are either dominant agonists (antipsychotic for mGluR2 and propsychotic for 2AR) or inverse agonists (antipsychotic for 2AR and propsychotic for mGluR2).

Inverse-Agonist Upmodulation Occurs in Mouse Frontal Cortex

To study the relevance of mGluR2/2AR heteromer signaling in vivo, we examined the pattern of G protein coupling in mouse frontal cortex, a region that plays an important role in schizophrenia and antipsychotic action (González-Maeso and Sealfon, 2009). We first measured the mGluR2/2AR complex-dependent upmodulation of Gi signaling by a 2AR inverse agonist. Membrane preparations from mouse frontal cortex were incubated with the inverse agonist clozapine or the neutral antagonist methysergide (Figures S4D and S4E), together with DCG-IV, a selective mGluR2/3 agonist. Clozapine increased the DCG-IV-mediated Gi signaling (Figure 5A), whereas methysergide did not significantly affect Gi signaling (Figure 5B). Furthermore, clozapine failed to increase the DCG-IV-mediated Gi signaling in frontal cortex membrane preparations from 2AR knockout (KO, *Htr2a*$^{-/-}$) mice (Figure S6C; see also Figures S6A and S6B for LY37-dependent activation of Gq in wild-type but not in 2AR-KO mouse frontal cortex).

We also tested the mGluR2 inverse-agonist upmodulation of Gq signaling in cortical primary cultures. Stimulation of Gq signaling in neurons is known to elicit a transient increase of intracellular calcium via an IP_3-mediated Ca^{2+} release from the endoplasmic reticulum (ER) that can be recorded using fluorescent calcium-sensitive dyes (Pichon et al., 2010). As predicted,

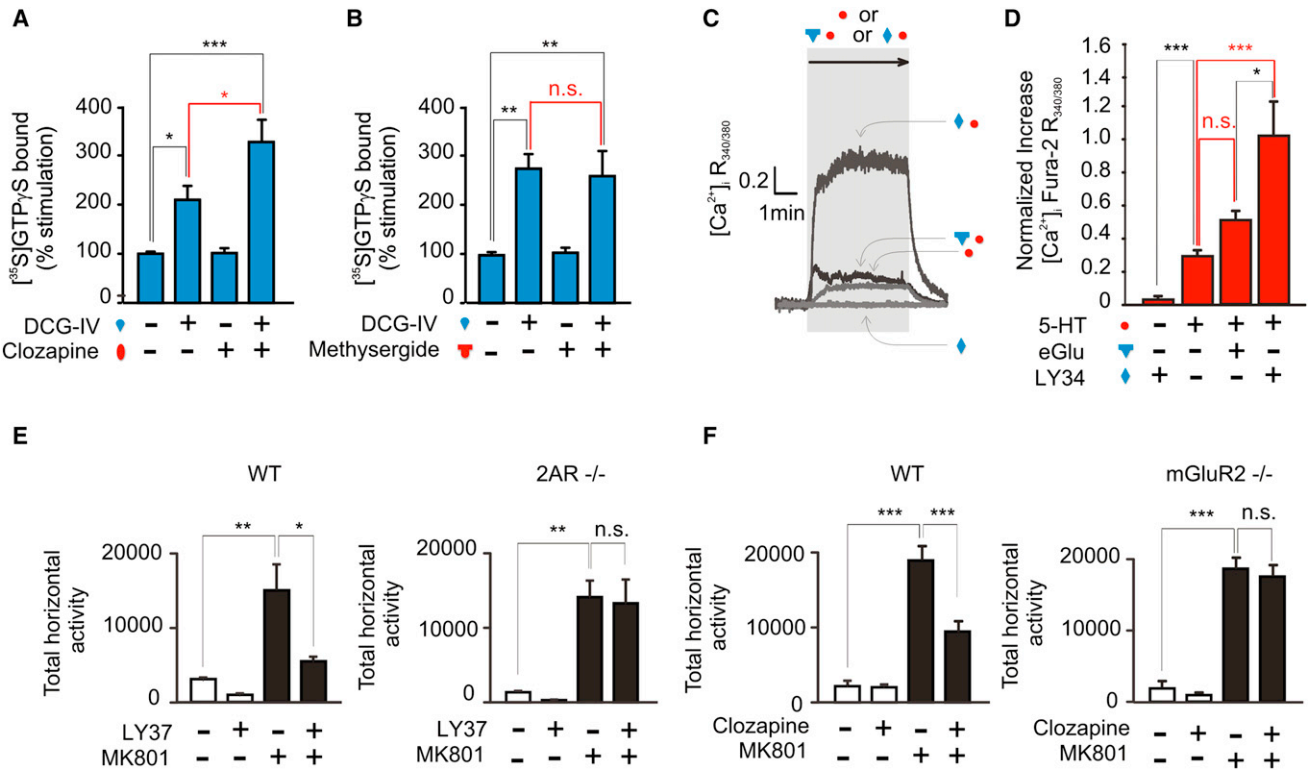

Figure 5. Upmodulation of Gq Signaling by LY34 and Gi Signaling by Clozapine in Mouse Frontal Cortex

DCG IV-stimulated [^{35}S]GTPγS binding in mouse frontal cortex membranes followed by immunoprecipitation with anti-Gαi antibody in the presence of clozapine (A), methysergide (B), or vehicle. Activation of Gi was accomplished by DCG IV (10 μM). Data represent mean ± SEM (*$p < 0.05$, **$p < 0.01$, ***$p < 0.001$, n.s.: not significant) (see also Figure S6C).

(C) Representative traces of 5-HT-evoked elevation of intracellular calcium in mouse cortical neurons as detected by ratiometric Fura-2 measurements. Measurements were obtained with 200 μM LY34 alone, 100 μM 5-HT (5-HT) alone, 100 μM 5-HT together with 200 μM eGlu (mGluR2 neutral antagonist), and 100 μM 5-HT together with 200 μM LY34 (mGluR2 inverse agonist).

(D) Bar graph summary of measured Fura-2 $R_{340/380}$ change. Traces were normalized to the basal level, the steady-state fluorescence before perfusion of drugs. Data are mean ± SEM (*$p < 0.05$, ***$p < 0.001$, n.s.: not significant).

(E) Summary bar graphs (mean ± SEM) of the total MK801-induced locomotion as a summation of horizontal activity from t = 30 min to t = 120 min. Injection time was at t = 0 min. Wild-type (WT, left) and 2AR-KO (right) mice were administered LY37 (5 mg/kg) or vehicle, followed by MK801 (0.5 mg/kg) or vehicle (N = 5–6).

(F) Wild-type mice were administered clozapine (1.5 mg/kg) or vehicle, followed by MK801 (0.5 mg/kg) or vehicle (left). mGluR2-KO mice were administered clozapine (1.5 mg/kg) or vehicle (right) (*$p < 0.05$, **$p < 0.01$, ***$p < 0.001$, n.s.: not significant).

LY34 was able to boost the 5-HT response nearly 5-fold (Figures 5C and 5D) but showed no response alone. In contrast, coapplication of the mGluR2 neutral antagonist eGlu with 5-HT did not elicit a significant increase in intracellular calcium (Figures 5C and 5D).

These data provide evidence that the effects of inverse agonists that bind 2AR or mGluR2 and boost their heteromeric partner receptor's signaling occur in cortical neurons in vivo (Figures 5A–5D).

2AR and mGluR2 Are Both Necessary for Antipsychotic-like Behavior in Mice

How do the antipsychotic drugs LY37 and clozapine influence behaviors? We determined the effects of the mGluR2/3 agonist LY37 on locomotor behavior precipitated by treatment with MK801 (Figure 5E). Noncompetitive NMDA receptor antagonists, such as phencyclidine (PCP) and ketamine, are used to model schizophrenia in rodents because of their capacity to evoke human behaviors similar to those observed in patients (Morris et al., 2005; Mouri et al., 2007; Patil et al., 2007). The potent and selective noncompetitive NMDA receptor antagonist MK801 (dizocilpine) can also elicit similar symptoms (Reimherr et al., 1986). Activation of mGluR2, but not mGluR3, by LY37 has been shown to reduce hyperlocomotion induced by noncompetitive NMDA antagonists in mouse models of schizophrenia (Woolley et al., 2008). MK801-stimulated locomotor activity in wild-type and 2AR-KO mice was indistinguishable. MK801-stimulated activity was significantly attenuated by LY37 in wild-type mice, but not in 2AR-KO (*Htr2a*$^{-/-}$) or mGluR2-KO (*Grm2*$^{-/-}$) mice (Figures 5E and S7B).

We next tested the role of mGluR2 in the antipsychotic-like effect induced by the atypical antipsychotic clozapine. Because clozapine binds with high affinity to 2ARs, and with lower affinity to dopamine D2 receptors (Meltzer et al., 1989), we first established the lowest dose of clozapine that induced an antipsychotic-like effect in mice (Figure S7A). The locomotor activity

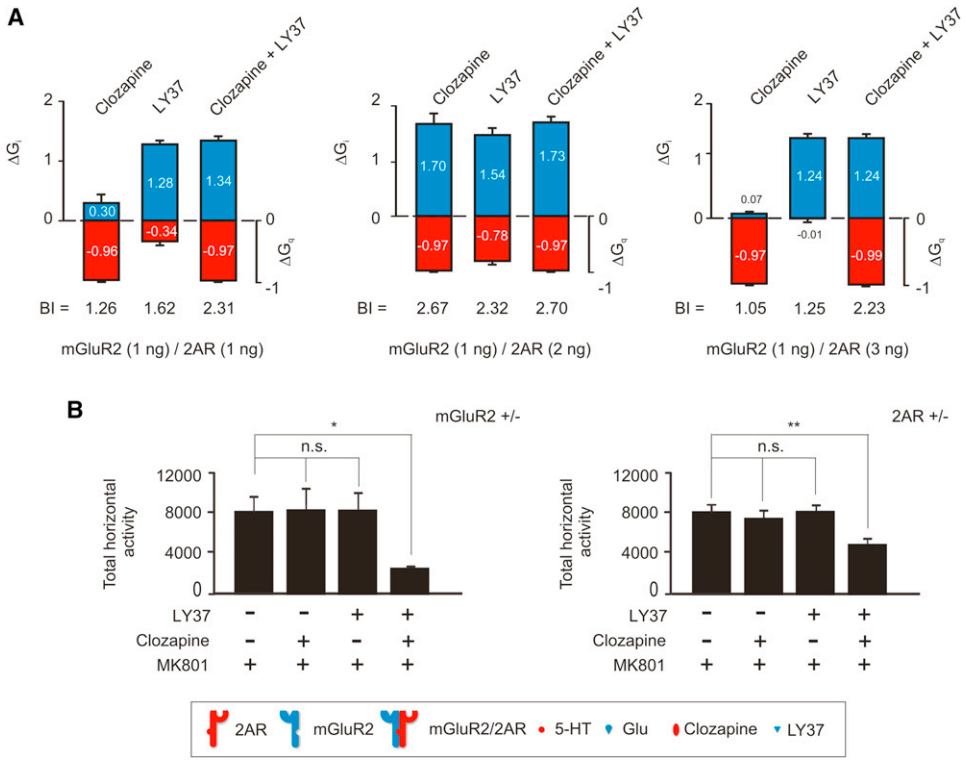

Figure 6. Control of BI through a Drug Combination Approach

(A) BI calculations at 50 μM concentrations of ligands. ΔGi referenced to the homomeric mGluR2 (1 ng of mRNA) response to 1 μM Glu and ΔGq referenced to the homomeric 2AR (2 ng of RNA) response to 1 μM 5-HT and 1 μM Glu. Responses to a concentration of 50 μM clozapine, LY37, or LY37 together with clozapine were measured in oocytes injected with 1 ng mGluR2 mRNA and 1 ng (left), 2 ng (center), and 3 ng (right) 2AR mRNA, respectively. Data are mean ± SEM.

(B) Summary bar graphs (mean ± SEM) of the total MK801-induced locomotion as a summation of horizontal activity from t = 30 min to t = 120 min. Injection time was at t = 0 min. mGluR2 heterozygotes (mGluR2$^{+/-}$) (left) and 2AR heterozygotes (right) are shown. Mice were administered vehicle, clozapine (1.5 mg/kg), LY37 (5 mg/kg), or both LY37 and clozapine, followed by MK801 (0.5 mg/kg) (N = 5–6). (*p < 0.05, n.s.: not significant).

induced by MK801 was similar in wild-type and mGluR2-KO mice. Notably, pretreatment with 1.5 mg/kg clozapine significantly decreased the MK801-stimulated locomotion in wild-type mice but not mGluR2-KO mice (Figure 5F), and this treatment had no effect on 2AR-KO mice (Figure S7C; see also Figures S7A–S7C). Although our results are consistent with the absence of antipsychotic-like behavioral effects of methysergide (compare Figure 5F for clozapine with Figures S7D and S7E for methysergide), they do not exclude the possibility that the absence of antipsychotic-like effects of LY37 in 2AR-KO may be affected by the lower expression of mGluR2 in 2AR-KO mice (González-Maeso et al., 2008; Moreno et al., 2011). Coinjection of LY37 and clozapine (1.5 mg/kg) did not affect the MK801-dependent locomotor response in either mGluR2-KO or 2AR-KO mice (data not shown). Together, these findings demonstrate that the mGluR2-dependent antipsychotic-like behavioral response of LY37 requires the expression of the 2AR, and that the corresponding 2AR-dependent effect of clozapine requires the expression of mGluR2.

A Drug Combination Approach to Control Psychotic-like Behavior

Recent preclinical findings suggest that coadministration of suboptimal doses of atypical and Glu antipsychotics results in robust therapeutic-like behavioral effects and reduced unwanted side effects (Uslaner et al., 2009). We postulated that alterations in 2AR and mGluR2 expression levels in our system (Figures 1F and S3D) may model the alterations in 2AR and mGluR2 ratios observed in postmortem brain samples from untreated schizophrenic patients (González-Maeso et al., 2008). We asked whether coadministration of clozapine (a 2AR inverse agonist) with LY37 (a mGluR2 dominant agonist) compensates for alterations in Gi-Gq balance caused by suboptimal expression ratios of the two receptors. To this end, we injected clozapine with LY37 and determined the BI. Figure 6A shows the ΔGi and ΔGq values obtained in response to clozapine, LY37, and LY37 together with clozapine. Coadministration of the two drugs increased significantly the BI in both suboptimal cases (left and right panels) compared to the optimal case (middle panel). These results reveal that coadministration of LY37 and clozapine can compensate for the loss in signaling capacity that is likely to result from decreased mGluR2/2AR heteromeric formation, as cross-signaling is decreased in suboptimal signaling receptor ratios.

Behavioral experiments showed that administration of either clozapine or LY37 in mGluR2 or 2AR heterozygote mice did not affect the MK801-dependent locomotor response (Figure 6B). However, coadministration of both antipsychotics

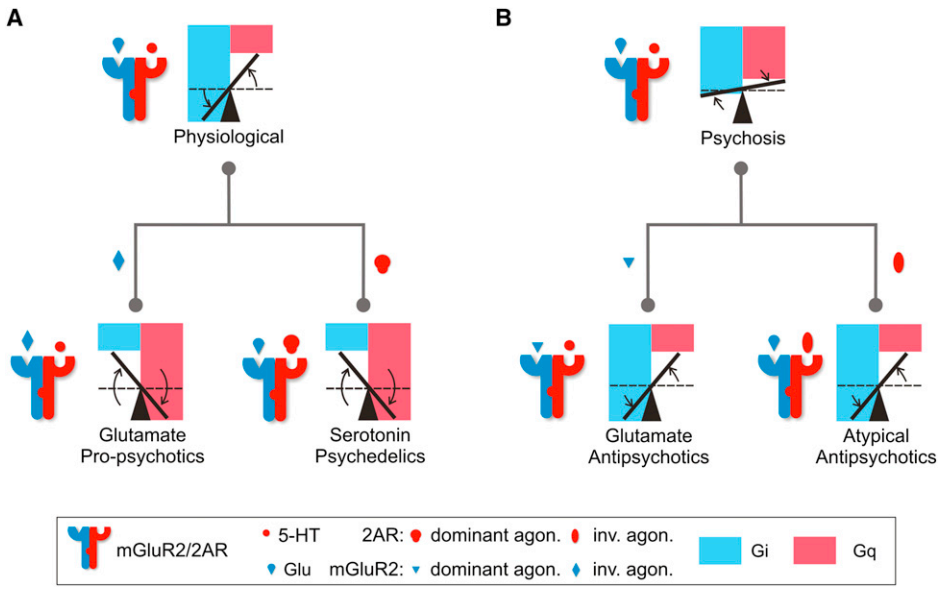

Figure 7. Gi-Gq Balance Model of the Mechanism of Action of Antipsychotic and Psychedelic Drugs through the mGluR2/2AR Complex

Formation of the receptor complex establishes an optimal Gi-Gq balance in response to Glu and 5-HT (increase in Gi, decrease in Gq).

(A) Psychedelics (LY34 and DOI) invert the balance (strong Gi decrease, strong Gq increase).

(B) Disruption of the optimal balance in psychotic states (decrease in Gi, increase in Gq) can be compensated for by antipsychotics (LY37, clozapine, and risperidone) that recover the Gi-Gq balance (increasing Gi and decreasing Gq).

in mGluR2 or 2AR heterozygotes significantly decreased the MK801-stimulated locomotor activity (Figure 6B). These results suggest that a combination of mGluR2 dominant agonists with 2AR inverse agonists is likely to synergize in vivo to achieve an optimal signaling ratio in cases where a suboptimal Gi-Gq signaling balance exists.

DISCUSSION

Previous work demonstrated that mGluR2 and 2AR form a functional heteromeric complex through which hallucinogenic drugs cross-signal to the Gi-coupled receptor (González-Maeso et al., 2008). It was not clear how the heteromeric complex signaled in response to ligands binding to either receptor and whether the differential pharmacology of this GPCR heteromer could be considered widely as a tractable therapeutic target for psychotic behavior. Our current study indicates that the mGluR2/2AR heteromer establishes a Gi-Gq balance in response to endogenous ligands (e.g., Glu and 5-HT). We utilized a simple metric, the BI, that quantifies the change in Gi (increase) and Gq (decrease) signaling upon heteromerization relative to the homomeric signaling levels.

The BI can be modulated either by dominant agonists that take control over their counterpart receptors or by inverse agonists that lift this control. This establishes a map between the ligand input to the heteromer (e.g., agonist/agonist, dominant agonist/agonist, neutral antagonist/agonist, inverse agonist/agonist) and its signaling output in terms of how specific ligands affect the BI. Our results are in agreement with results from a GPCR complex of D2 receptor homomers coupled to a single Gi protein subunit (Han et al., 2009). Our study further extends these previous findings and demonstrates a signaling crosstalk between the 2AR and mGluR2, which are individually coupled to two different subtypes of G proteins (Gq and Gi). Our data indicate that signaling crosstalk through the mGluR2/2AR heterocomplex may be a causal mechanism for the induction of cellular and behavioral responses that differ from those of mGluR2 and 2AR homomers.

In our model (Figure 7), psychedelics invert the signaling balance through the complex (Gi signaling decreases, whereas Gq signaling increases, thus decreasing the BI), tipping the balance from being in favor of Gi signaling (normal complex) to being in favor of Gq signaling (propsychotic) (Figure 7A). Similarly, disease states involving psychosis, such as schizophrenia, would be expected to be associated with a variable disruption of the Gi-Gq balance (i.e., decrease in Gi, increase in Gq, and decrease in BI) (Figure 7B), consistent with the mGluR2 downregulation and 2AR upregulation observed in untreated schizophrenic patients (González-Maeso et al., 2008). Such disruption would be reversed by antipsychotics that recover the Gi-Gq balance again in favor of Gi as in the normal complex (i.e., increasing Gi and decreasing Gq, thus increasing the BI) (Figure 7B). Because the Gi-Gq balance is the regulated variable predicting psychotic state, it is not surprising that inverse agonists on the 2AR side and strong agonists on the mGluR2 side are the most effective antipsychotics. The present study also suggests a unifying mechanism of action of atypical antipsychotics and the new glutamate antipsychotics. Our findings suggest inverse agonism as a common feature of 2AR ligands with antipsychotic properties. We show that dysregulation of an optimal ratio of mGluR2 to 2AR expression via injection of different mRNA ratios greatly decreases BI values, and single

application of 2AR inverse agonists or mGluR2 dominant agonists may not push the BI into the therapeutic range (see Figure 4). Yet coadministration of the most effective mGluR2 and 2AR drugs yields BI values in the therapeutic range (Figure 6). These findings in heterologous systems were paralleled in vivo using heterozygous mice for 2AR or mGluR2: coinjection of both clozapine and LY37 was needed to decrease the MK801-dependent locomotor activity. In some schizophrenic patients, atypical antipsychotics produce complete remission of psychotic symptoms. However, two-thirds of schizophrenic patients are considered treatment resistant, with persistent psychotic and other symptoms despite the optimal use of available antipsychotic medications (Lieberman et al., 2005). The absence of antipsychotic-like behavioral effect by injection of either LY37 or clozapine in 2AR or mGluR2 heterozygous mice, but not in the same mice coinjected with LY37 and clozapine, points toward potential beneficial use of combination therapy in treatment-resistant schizophrenia.

The metric (BI) that we provide allows quantification and prediction of anti-/propsychotic effects of new drugs acting through the mGluR2/2AR receptor heterocomplex. Although long-term effects of drugs targeting mGluR2/2AR signaling are not taken into account in the way we have estimated the BI metric, the ability of this scale to predict appropriately the most effective anti- and propsychotic drugs acting through the receptor heterocomplex makes it a promising tool in predicting the efficacy of new drugs. This metric, as well as structural insights from ligand-specific heteromeric conformations, could be used extensively for screening new compounds with potential antipsychotic effects.

Our results pave the way toward a new understanding of the cellular signaling, function, and pharmacology of other heteromeric GPCRs that have been implicated as therapeutic targets for the treatment of disease (Milligan, 2009). Provided that the receptor complex signaling output can classify accurately the behavior of drugs targeting the complex and used to treat disease, the case of the mGluR2/2AR complex can serve as a guiding example of development of therapeutic potency scales that can be used to classify existing drugs and predict the behavior of novel ones. Because the most effective antipsychotic drugs targeting the mGluR2/2AR complex all gave the highest BI values, it is likely that somehow signaling through this complex is uniquely coupled to specific targets. The mechanism of such signaling specificity as well as the detailed actions of Gi versus Gq signaling through the mGluR2/2AR complex, aiming to achieve a homeostatic balance that ensures a normal nonpsychotic state, are likely to become an active pursuit of future studies.

EXPERIMENTAL PROCEDURES

Drugs, Molecular Constructs, Analysis of mGluR2 and 2AR Protein Levels, and Surface Expression Assays

See Extended Experimental Procedures for details on all of these.

Expression of Recombinant Proteins in *Xenopus* Oocytes

Oocytes were isolated and microinjected with equal volumes (50 nl), as previously described (Lopes et al., 2002). In all two-electrode voltage-clamp experiments (TEVC), oocytes were injected with 1 ng of mGluR2, 2 ng of mGluR2ΔTM4,5, 2 ng of mGluR3, 2 ng of mGluR3ΔTM4,5, 2 ng of 2AR, 2 ng of GIRK4*, 2 ng of IRK3, 1 ng of PTX, or 4 ng of RGS2 and were maintained at 18°C for 1–4 days before recording.

TEVC Recording and Analysis

Whole-cell currents were measured by conventional TEVC with a GeneClamp 500 amplifier (Axon Instruments, Union City, CA, USA), as previously reported. A high-potassium (HK) solution was used to superfuse oocytes (96 mM KCl, 1 mM NaCl, 1 mM $MgCl_2$, 5 mM KOH/HEPES, pH 7.4) to obtain a reversal potential for potassium (E_K) close to zero.

Inwardly rectifying potassium currents through GIRK4* and IRK3 were obtained by clamping the cells at −80 mV. In order to isolate Gi, GIRK4* was coinjected with RGS2 in order to eliminate the Gq component in the current. Basal IRK3 and GIRK4* currents were defined as the difference between inward currents obtained at −80 mV in the presence of 3 mM $BaCl_2$ in HK solution and those in the absence of Ba^{2+} and measured for each trace. Current inhibition and current activation were measured respectively and normalized to basal current to compensate for size variability in oocytes.

Computational Methods

Molecular modeling: Because there are no available crystal structures of the 2AR or mGluR2 available to date, we generated initial molecular models of these two receptors. Specifically, we built initial inactive conformations of 2AR or mGluR2 using a combination of homology modeling for the TM helices and an ab initio loop prediction approach implemented in the Rosetta 2.2 code (Wang et al., 2007) for the loop regions of the receptors. According to specific structural and functional similarities, the β2-adrenergic (PDB 2RH1 (Cherezov et al., 2007) or -rhodopsin (PDB 1U19 (Okada et al., 2004)) crystal structures were used as structural templates for the homology modeling of the TM regions of 2AR or mGluR2, respectively. We generated activation pathways for each receptor using the adiabatic-biased MD (ABMD) algorithm (Paci and Karplus, 1999) and a recently published simulation protocol (see Provasi et al., 2011 for details). Free-energy values were calculated using a Monte Carlo scheme.

(see Extended Experimental Procedures for additional details.)

Experimental Animals

Experiments were performed on adult (8- to 12-week-old) male 129S6/SvEv mice. 2AR-KO mice have been previously described (González-Maeso et al., 2007). mGluR2-KO mice were obtained from the RIKEN BioResource Center, Japan (see reference Yokoi et al., 1996 for details) and backcrossed for at least ten generations onto a 129S6/SvEv background. All subjects were offspring of heterozygote breeding. For experiments involving genetically modified mice, 2AR wild-type or mGluR2 wild-type littermates were used as controls. Animals were housed for 12 hr light/dark cycles at 23°C with food and water ad libitum. The Institutional Animal Use and Care Committee approved all experimental procedures at the Mount Sinai School of Medicine and Virginia Commonwealth University.

Measurement of Intracellular Ca^{2+}

Measurement of intracellular free calcium was performed as described in the literature with minor modifications (Pichon et al., 2010) (see Extended Experimental Procedures for details).

Coimmunoprecipitations and [^{3}H]Ketanserin and [^{35}S]GTPγS Binding Assays

Mouse frontal cortex membrane preparations and binding assays were performed as previously described with minor modifications (González-Maeso et al., 2008) (see Extended Experimental Procedures for details).

Cortical Primary Cultures and Immunocytochemistry

Mouse cortical primary neurons were cultured as previously reported (González-Maeso et al., 2008).

(See Extended Experimental Procedures for details.)

Behavioral Studies

Locomotor and head-twitch behavioral studies were performed as previously described (González-Maeso et al., 2008). Motor function was assessed with

a computerized three-dimensional activity monitoring system (AccuScanInstruments). The activity monitor has 32 infrared sensor pairs, with 16 along each side spaced 2.5 cm apart. The system determines motor activity on the basis of the frequency of interruptions to infrared beams traversing the x, y, and z planes. Total distance (cm) traveled and vertical activity were determined automatically from the interruptions of beams in the horizontal and vertical planes, respectively.

Calculation of Gi-Gq Balance Recovery and Loss

The total Gi-Gq balance achieved by the mGluR2/2AR heteromer in the presence of a drug was calculated with the following equation:

$$\text{Total balance} = x\ BI_d + BI_r(1 - x)$$

where x is the fraction of heteromer that binds the drug, BI_d is the balance index of the drug at a fixed concentration, and BI_r is the reference balance index of the complex (1.45).

In the absence of drug ($x = 0$), the total balance achieved will be BI_r (1.45). If the drug has a $BI_d = BI_r$, the total Gi-Gq balance is also BI_r (1.45) for any fraction x of drug-bound heteromer.

In a state where the mGluR2/2AR heteromer is signaling at a $BI < BI_r$ (disease state), a drug with a $BI_d > BI_r$ will be able to compensate for the total Gi-Gq balance loss and reestablish a total balance of 1.45 (BI_r), if BI_d is sufficiently large.

The Gi-Gq balance recovery (R) was calculated with the following equation:

$$R = 100 \cdot \left[\left(\frac{\text{Total balance}}{BI_r} \right) - 1 \right]$$

This value expressed as a percentage indicates the amount of Gi-Gq balance that could be recovered by a drug with a balance index BI_d. It is determined by the difference between the total balance achieved in the presence of the drug compared to BI_r. A positive Gi-Gq balance (total balance > BI_r) indicates that the drug is able to recover Gi-Gq balance (e.g., a drug with a BI_d of 2.3 with a fractional occupancy $x = 0.5$ will have a total balance of 1.875, which will allow recovery up to ~30% loss from the reference level of 1.45). A negative Gi-Gq balance (total balance < BI_r) indicates that the drug induces a loss in balance (e.g., a drug with a BI_d of 0.315 with a fractional occupancy $x = 0.5$ will have a total balance of 0.315, which will result in ~80% loss from the reference level of 1.45).

In order to compare drugs, we established an arbitrary reference level of fractional occupancy of the heteromer by the drug ($x = 0.5$). This allowed us to establish the differences in the ability of the drugs to recover or lose the Gi-Gq balance based on their BI at equal conditions. Changes in the fractional occupancy used for comparison (e.g., $x = 0.25$) changed the magnitude but not the relative order in the classification of the drugs shown in Figure 4.

Statistical Methods

Statistical significance of behavioral experiments involving four groups and two treatments was assessed by two-factor ANOVA followed by Bonferroni's post-hoc test. Statistical significance of behavioral experiments involving one treatment was assessed by Student's t test.

Each electrophysiological experiment in *Xenopus* oocytes was performed in two batches. Every group in each experiment was tested in both batches. Data for both batches were compiled (n = 8–16), and one-way ANOVA tests applied followed by a multiple comparison procedure using Tukey's honestly significant difference test.

Intracellular calcium measurements were performed in three different isolations. Data for all isolations were compiled (n = 7–11), and one-way ANOVA tests applied followed by a multiple comparison procedure using Tukey's honestly significant difference test.

[^{3}H]ketanserin binding experiments were performed 3–5 times in duplicate/triplicate. A one-site model versus a two-site model, as a better description of the data, was determined by F test. [^{35}S]GTPγS binding experiments were performed three times in triplicate. Two-way ANOVA tests were applied to the compiled data followed by a Bonferroni's post-hoc test.

SUPPLEMENTAL INFORMATION

Supplemental information includes Extended Experimental Procedures, seven figures, and two tables and can be found with this article online at doi:10.1016/j.cell.2011.09.055.

ACKNOWLEDGMENTS

The authors thank Sophia Gruszecki, Heikki Vaananen, Dr. Jian Yang, and Dr. Basil Hanss for *Xenopus* oocyte isolation and are grateful to Dr. Kurt Hauser for his support with the cortical primary neuronal cultures and Dr. J.A. Gingrich for his gift of 5HT2A-KO mice. The authors are also thankful to Drs. M. Scott Bowers, Louis J. De Felice, Frank Guarnieri (Virginia Commonwealth University), Lakshmi Devi (Mount Sinai School of Medicine), Jonathan Javitch (Columbia University), George Liapakis (University of Crete, Greece), and Herbert Meltzer (Vanderbilt University) for critical feedback on the manuscript and to members of the Logothetis lab for useful feedback throughout this project. D.E.L. was partly supported for this work by NIH grant HL59949. J.G.-M. was supported by NIH grant 5R01MH084894, as well as NARSAD, Dainippon Sumitomo Pharma, and the Maltz Family Foundation Award. M.F. was supported by NIH grants MH084894, MH091360, and DA026434. The computations were supported in part by the National Science Foundation through TeraGrid advanced computing resources provided by the Texas Advanced Computing Center under grant TG-MCB080109N. J.L.M. was the recipient of a postdoctoral fellowship from Ministerio de Ciencia e Innovación, Spain. R.M. was supported by NIH grant F30HL097582. J.M.E. was supported by NIH grants SRC1DA02811202 and 1R01DA02694702.

Received: November 19, 2010
Revised: August 16, 2011
Accepted: September 30, 2011
Published: November 23, 2011

REFERENCES

Aloyo, V.J., Berg, K.A., Spampinato, U., Clarke, W.P., and Harvey, J.A. (2009). Current status of inverse agonism at serotonin2A (5-HT2A) and 5-HT2C receptors. Pharmacol. Ther. *121*, 160–173.

Barela, A.J., Waddy, S.P., Lickfett, J.G., Hunter, J., Anido, A., Helmers, S.L., Goldin, A.L., and Escayg, A. (2006). An epilepsy mutation in the sodium channel SCN1A that decreases channel excitability. J. Neurosci. *26*, 2714–2723.

Barducci, A., Bussi, G., and Parrinello, M. (2008). Well-tempered metadynamics: a smoothly converging and tunable free-energy method. Phys. Rev. Lett. *100*, 020603.

Bespalov, A., Jongen-Rêlo, A.L., van Gaalen, M., Harich, S., Schoemaker, H., and Gross, G. (2007). Habituation deficits induced by metabotropic glutamate receptors 2/3 receptor blockade in mice: reversal by antipsychotic drugs. J. Pharmacol. Exp. Ther. *320*, 944–950.

Bonomi, D., Branduardi, G., and Bussi, C. (2009). PLUMED: A portable plugin for free-energy calculations with molecular dynamics. Comput. Phys. Commun. *180*, 1961–1972.

Branduardi, D., Gervasio, F.L., and Parrinello, M. (2007). From A to B in free energy space. J. Chem. Phys. *126*, 054103.

Carriba, P., Navarro, G., Ciruela, F., Ferré, S., Casadó, V., Agnati, L., Cortés, A., Mallol, J., Fuxe, K., Canela, E.I., et al. (2008). Detection of heteromerization of more than two proteins by sequential BRET-FRET. Nat. Methods *5*, 727–733.

Cherezov, V., Rosenbaum, D.M., Hanson, M.A., Rasmussen, S.G., Thian, F.S., Kobilka, T.S., Choi, H.J., Kuhn, P., Weis, W.I., Kobilka, B.K., and Stevens, R.C. (2007). High-resolution crystal structure of an engineered human beta2-adrenergic G protein-coupled receptor. Science *318*, 1258–1265.

Du, X., Zhang, H., Lopes, C., Mirshahi, T., Rohacs, T., and Logothetis, D.E. (2004). Characteristic interactions with phosphatidylinositol 4,5-bisphosphate

determine regulation of kir channels by diverse modulators. J. Biol. Chem. *279*, 37271–37281.

Egan, C.T., Herrick-Davis, K., and Teitler, M. (1998). Creation of a constitutively activated state of the 5-hydroxytryptamine2A receptor by site-directed mutagenesis: inverse agonist activity of antipsychotic drugs. J. Pharmacol. Exp. Ther. *286*, 85–90.

Ernst, O.P., Gramse, V., Kolbe, M., Hofmann, K.P., and Heck, M. (2007). Monomeric G protein-coupled receptor rhodopsin in solution activates its G protein transducin at the diffusion limit. Proc. Natl. Acad. Sci. USA *104*, 10859–10864.

González-Maeso, J., and Sealfon, S.C. (2009). Psychedelics and schizophrenia. Trends Neurosci. *32*, 225–232.

González-Maeso, J., Rodríguez-Puertas, R., and Meana, J.J. (2002). Quantitative stoichiometry of G-proteins activated by mu-opioid receptors in postmortem human brain. Eur. J. Pharmacol. *452*, 21–33.

González-Maeso, J., Weisstaub, N.V., Zhou, M., Chan, P., Ivic, L., Ang, R., Lira, A., Bradley-Moore, M., Ge, Y., Zhou, Q., et al. (2007). Hallucinogens recruit specific cortical 5-HT(2A) receptor-mediated signaling pathways to affect behavior. Neuron *53*, 439–452.

González-Maeso, J., Ang, R.L., Yuen, T., Chan, P., Weisstaub, N.V., López-Giménez, J.F., Zhou, M., Okawa, Y., Callado, L.F., Milligan, G., et al. (2008). Identification of a serotonin/glutamate receptor complex implicated in psychosis. Nature *452*, 93–97.

Han, Y., Moreira, I.S., Urizar, E., Weinstein, H., and Javitch, J.A. (2009). Allosteric communication between protomers of dopamine class A GPCR dimers modulates activation. Nat. Chem. Biol. *5*, 688–695.

He, C., Zhang, H., Mirshahi, T., and Logothetis, D.E. (1999). Identification of a potassium channel site that interacts with G protein betagamma subunits to mediate agonist-induced signaling. J. Biol. Chem. *274*, 12517–12524.

He, C., Yan, X., Zhang, H., Mirshahi, T., Jin, T., Huang, A., and Logothetis, D.E. (2002). Identification of critical residues controlling G protein-gated inwardly rectifying K(+) channel activity through interactions with the beta gamma subunits of G proteins. J. Biol. Chem. *277*, 6088–6096.

Hof, P.R., et al. (2000). Comparative Cytoarchitectonic Atlas of the C57BL/6 and 129/Sv Mouse Brains (Amsterdam: Elsevier).

Kenakin, T. (2002). Efficacy at G-protein-coupled receptors. Nat. Rev. Drug Discov. *1*, 103–110.

Kinon, B.J., Zhang, L., Millen, B.A., Osuntokun, O.O., Williams, J.E., Kollack-Walker, S., Jackson, K., Kryzhanovskaya, L., and Jarkova, N.; and the HBBI Study Group. (2011). A multicenter, inpatient, phase 2, double-blind, placebo-controlled dose-ranging study of LY2140023 monohydrate in patients with DSM-IV schizophrenia. J. Clin. Psychopharmacol. *31*, 349–355.

Lieberman, J.A., Stroup, T.S., McEvoy, J.P., Swartz, M.S., Rosenheck, R.A., Perkins, D.O., Keefe, R.S., Davis, S.M., Davis, C.E., Lebowitz, B.D., et al; Clinical Antipsychotic Trials of Intervention Effectiveness (CATIE) Investigators. (2005). Effectiveness of antipsychotic drugs in patients with chronic schizophrenia. N. Engl. J. Med. *353*, 1209–1223.

Lopes, C.M., Zhang, H., Rohacs, T., Jin, T., Yang, J., and Logothetis, D.E. (2002). Alterations in conserved Kir channel-PIP2 interactions underlie channelopathies. Neuron *34*, 933–944.

Lopez-Gimenez, J.F., Canals, M., Pediani, J.D., and Milligan, G. (2007). The alpha1b-adrenoceptor exists as a higher-order oligomer: effective oligomerization is required for receptor maturation, surface delivery, and function. Mol. Pharmacol. *71*, 1015–1029.

Meltzer, H.Y., and Huang, M. (2008). In vivo actions of atypical antipsychotic drug on serotonergic and dopaminergic systems. Prog. Brain Res. *172*, 177–197.

Meltzer, H.Y., Matsubara, S., and Lee, J.C. (1989). Classification of typical and atypical antipsychotic drugs on the basis of dopamine D-1, D-2 and serotonin2 pKi values. J. Pharmacol. Exp. Ther. *251*, 238–246.

Milligan, G. (2009). G protein-coupled receptor hetero-dimerization: contribution to pharmacology and function. Br. J. Pharmacol. *158*, 5–14.

Moreno, J.L., Sealfon, S.C., and González-Maeso, J. (2009). Group II metabotropic glutamate receptors and schizophrenia. Cell. Mol. Life Sci. *66*, 3777–3785.

Moreno, J.L., Holloway, T., Albizu, L., Sealfon, S.C., and González-Maeso, J. (2011). Metabotropic glutamate mGlu2 receptor is necessary for the pharmacological and behavioral effects induced by hallucinogenic 5-HT2A receptor agonists. Neurosci. Lett. *493*, 76–79.

Morris, B.J., Cochran, S.M., and Pratt, J.A. (2005). PCP: from pharmacology to modelling schizophrenia. Curr. Opin. Pharmacol. *5*, 101–106.

Mouri, A., Noda, Y., Enomoto, T., and Nabeshima, T. (2007). Phencyclidine animal models of schizophrenia: approaches from abnormality of glutamatergic neurotransmission and neurodevelopment. Neurochem. Int. *51*, 173–184.

Okada, T., Sugihara, M., Bondar, A.N., Elstner, M., Entel, P., and Buss, V. (2004). The retinal conformation and its environment in rhodopsin in light of a new 2.2 A crystal structure. J. Mol. Biol. *342*, 571–583.

Oldham, W.M., and Hamm, H.E. (2008). Heterotrimeric G protein activation by G-protein-coupled receptors. Nat. Rev. Mol. Cell Biol. *9*, 60–71.

Paci, E., and Karplus, M. (1999). Forced unfolding of fibronectin type 3 modules: an analysis by biased molecular dynamics simulations. J. Mol. Biol. *288*, 441–444.

Patil, S.T., Zhang, L., Martenyi, F., Lowe, S.L., Jackson, K.A., Andreev, B.V., Avedisova, A.S., Bardenstein, L.M., Gurovich, I.Y., Morozova, M.A., et al. (2007). Activation of mGlu2/3 receptors as a new approach to treat schizophrenia: a randomized Phase 2 clinical trial. Nat. Med. *13*, 1102–1107.

Pichon, X., Wattiez, A.S., Becamel, C., Ehrlich, I., Bockaert, J., Eschalier, A., Marin, P., and Courteix, C. (2010). Disrupting 5-HT(2A) receptor/PDZ protein interactions reduces hyperalgesia and enhances SSRI efficacy in neuropathic pain. Mol. Ther. *18*, 1462–1470.

Provasi, D., Artacho, M.C., Negri, A., Mobarec, J.C., and Filizola, M. (2011). Ligand-induced modulation of the free-energy landscape of g protein-coupled receptors explored by adaptive biasing techniques. PLoS Comput. Biol. *7*, e1002193.

Reimherr, F.W., Wood, D.R., and Wender, P.H. (1986). The use of MK-801, a novel sympathomimetic, in adults with attention deficit disorder, residual type. Psychopharmacol. Bull. *22*, 237–242.

Rives, M.L., Vol, C., Fukazawa, Y., Tinel, N., Trinquet, E., Ayoub, M.A., Shigemoto, R., Pin, J.P., and Prézeau, L. (2009). Crosstalk between GABAB and mGlu1a receptors reveals new insight into GPCR signal integration. EMBO J. *28*, 2195–2208.

Rosenbaum, D.M., Rasmussen, S.G., and Kobilka, B.K. (2009). The structure and function of G-protein-coupled receptors. Nature *459*, 356–363.

Ross, C.A., Margolis, R.L., Reading, S.A., Pletnikov, M., and Coyle, J.T. (2006). Neurobiology of schizophrenia. Neuron *52*, 139–153.

Urizar, E., Yano, H., Kolster, R., Galés, C., Lambert, N., and Javitch, J.A. (2011). CODA-RET reveals functional selectivity as a result of GPCR heteromerization. Nat. Chem. Biol. *7*, 624–630.

Uslaner, J.M., Smith, S.M., Huszar, S.L., Pachmerhiwala, R., Hinchliffe, R.M., Vardigan, J.D., and Hutson, P.H. (2009). Combined administration of an mGlu2/3 receptor agonist and a 5-HT 2A receptor antagonist markedly attenuate the psychomotor-activating and neurochemical effects of psychostimulants. Psychopharmacology (Berl.) *206*, 641–651.

Vanommeslaeghe, K., Hatcher, E., Acharya, C., Kundu, S., Zhong, S., Shim, J., Darian, E., Guvench, O., Lopes, P., Vorobyov, I., and Mackerell, A.D., Jr. (2010). CHARMM general force field: A force field for drug-like molecules compatible with the CHARMM all-atom additive biological force fields. J. Comput. Chem. *31*, 671–690.

Vilardaga, J.P., Nikolaev, V.O., Lorenz, K., Ferrandon, S., Zhuang, Z., and Lohse, M.J. (2008). Conformational cross-talk between alpha2A-adrenergic and mu-opioid receptors controls cell signaling. Nat. Chem. Biol. *4*, 126–131.

Wang, C., Bradley, P., and Baker, D. (2007). Protein-protein docking with backbone flexibility. J. Mol. Biol. *373*, 503–519.

Weiner, D.M., Burstein, E.S., Nash, N., Croston, G.E., Currier, E.A., Vanover, K.E., Harvey, S.C., Donohue, E., Hansen, H.C., Andersson, C.M., et al. (2001). 5-hydroxytryptamine2A receptor inverse agonists as antipsychotics. J. Pharmacol. Exp. Ther. *299*, 268–276.

Whorton, M.R., Bokoch, M.P., Rasmussen, S.G., Huang, B., Zare, R.N., Kobilka, B., and Sunahara, R.K. (2007). A monomeric G protein-coupled receptor isolated in a high-density lipoprotein particle efficiently activates its G protein. Proc. Natl. Acad. Sci. USA *104*, 7682–7687.

Woolley, M.L., Pemberton, D.J., Bate, S., Corti, C., and Jones, D.N. (2008). The mGlu2 but not the mGlu3 receptor mediates the actions of the mGluR2/3 agonist, LY379268, in mouse models predictive of antipsychotic activity. Psychopharmacology (Berl.) *196*, 431–440.

Yokoi, M., Kobayashi, K., Manabe, T., Takahashi, T., Sakaguchi, I., Katsuura, G., Shigemoto, R., Ohishi, H., Nomura, S., Nakamura, K., et al. (1996). Impairment of hippocampal mossy fiber LTD in mice lacking mGluR2. Science *273*, 645–647.

Cell

EXTENDED EXPERIMENTAL PROCEDURES

Drugs

5-hydroxytryptamine (serotonin, 5-HT), 1-(2,5-dimethoxy-4-iodophenyl)-2-aminopropane (DOI), and (+)-MK801 hydrogen maleate (MK801) were purchased from Sigma-Aldrich. (1R,4R,5S,6R)-4-Amino-2-oxabicyclo[3.1.0]hexane-4,6-dicarboxylic acid (LY379268; LY37), (2S)-2-Amino-2-[(1S,2S)-2-carboxycycloprop-1-yl]-3-(xanth-9-yl) propanoic acid (LY341495; LY34), methysergide, clozapine, paliperidone (active compound of risperidone), ritanserin, (2S)-a-ethylglutamic acid (eGlu), and (2S,2′R,3′R)-2-(2′,3′-Dicarboxycyclopropyl) glycine (DCG-IV) were obtained from Tocris Cookson Inc. [^{35}S]GTPγS and [^{3}H]ketanserin were purchased from PerkinElmer Life and Analytical Sciences, Inc.

Molecular Constructs

PCR amplification and subcloning of 2AR, mGluR2, mGluR3, mGluR2Δ (mGluR2 chimera containing TM helices 4 and 5 of the mGluR3), and mGluR3Δ (mGluR3 chimera containing TM helices 4 and 5 of the mGluR2) into pcDNA3.1 was described previously (González-Maeso et al., 2008). The human 2AR, the human mGluR2, and the mGluR2Δ were digested with BamHI and NotI and subcloned into the pXOOM vector. The human mGluR3 and the mGluR3Δ chimeras were digested with EcoRI and NotI and subcloned into pXOOM (González-Maeso et al., 2008). The human RGS2 (University of Missouri-Rolla, UMR) was PCR-amplified using the primers RGS2/S (TTTTggatccATGCAAAGTGCTATGTTCTT) and RGS2/A (TTTTgcggccgcTCATGTAGCATGAGGCTCTG) and subcloned into the BamHI and NotI sites of pXOOM. Constructs subcloned into the pGEMHE vector with the active point mutants of the human Kir3.4, Kir3.4-S143T or Kir3.4*, Kir2.3 (IRK3) and Pertussis Toxin (PTX) subunit B were previously described (Vivaudou et al., 1997).

Surface Labeling of Oocytes

We engineered HA-tagged 2AR, mGluR2, mGluR3, mGluR2ΔTM4,5 and mGluR3ΔTM4,5 constructs as previously described (González-Maeso et al., 2002) and used an ELISA-based chemiluminescence assay adapted for oocytes. Oocytes were blocked for 30–60 min in experimental medium (ND96 with 1% bovine serum albumin (BSA)) at 4°C, labeled with 0.5 μg/ml rat monoclonal anti-HA antibody (3F10; Boehringer Mannheim) (overnight at 4°C), extensively washed at 4°C, and incubated with 2 μg/ml HRP-coupled secondary antibody (goat anti-rat) (in 1% BSA for 60 min). Cells were washed (experimental medium, 4°C) and transferred to ND96 without BSA. Individual oocytes were placed in 100 μl SuperSignal ELISA (Pierce) and incubated at room temperature for 1 min. Chemiluminescence was quantitated in a TD-20E luminometer (Turner Designs, CA, USA). As a control, we used noninjected oocytes.

Computational Methods

Conformational Sampling of Ligand-free 2AR or mGluR2

We used the crystal structures of the G protein-interacting opsin (PDB 3DQB [Scheerer et al., 2008]) and the nanobody-stabilized activated β2-adrenergic receptor (PDB 3PX0 [Rasmussen et al., 2011]) as target active conformations for mGluR2 and 2AR, respectively. The CHARMM27 force-field (MacKerell et al., 1998) was used to describe the receptors (along with the CMAP backbone energy correction (Mackerell et al., 2004)), as well as the lipids. All calculations were performed using NAMD 2.7 (Phillips et al., 2005), enhanced with the Plumed plug-in (Bonomi et al., 2009). Briefly, we carried out multiple 10 ns-long ABMD simulations in an explicit hydrated 1-palmitoyl-2-oleoyl-sn-glycero-3-phosphocholine (POPC)/10% cholesterol membrane bilayer with an elastic constant of 0.1 kJ/nm2 for each system. The ligand-free sampled conformations of either 2AR or mGluR2 were grouped using average linkage agglomerative hierarchical clustering based on the root mean square deviation (rmsd) of the TM domains, and path collective variables for metadynamics simulations were derived using the maximum number of clusters k that would define mono-dimensional paths for each receptor. To avoid rapid switching between clusters and to ensure all clusters were visited in a sequential fashion by the conformations of a given trajectory, we considered a maximum number of clusters k = 8.

Ligand Parameterization and Docking

Clozapine, methysergide, DOI were parameterized based on the General CHARMM force-field optimization protocol (Vanommeslaeghe et al., 2010). These ligands were docked into the initial inactive model of 2AR, using a standard Autodock 4.0 (Morris et al., 2009) protocol. Inferences from published experimental work on clozapine (Kanagarajadurai et al., 2009), methysergide (Roth et al., 1997), or DOI (Braden et al., 2006) binding were considered to select the most accurate initial binding poses of these ligands for further metadynamics simulations.

Metadynamics of Ligand-bound 2AR

Metadynamics simulations were performed on each ligand-bound 2AR system within an explicit environment, using as reaction coordinates path variables (Branduardi et al., 2007) describing the position along (s) and the distance from (z) the predetermined activation trajectories of the 2AR. A bias was added to the system using the well-tempered metadynamics algorithm (Barducci et al., 2008), with a deposition rate of 150 ps, an initial energy of the Gaussian bias of w = 0.1 kcal/mol, and a bias-factor of 10. Convergence of the reconstructed free-energy was monitored by checking the height of the Gaussian bias contributions as a function of simulation time, and the simulation was stopped after 150 ns.

Exploration of the Dimer Interfaces

To study which interfaces involving TM4 and/or TM5 helices are stabilized by the ligand-specific 2AR conformations, we carried out all-atom Monte Carlo simulations with an implicit membrane model. Focus on these helices was based on inferences from the literature on several GPCR complexes, as well as both published (González -Maeso et al., 2008) and unpublished data on 2AR and mGluR2. The receptors were described using the same force field used in the metadynamics simulations (MacKerell et al., 1998; Mackerell et al., 2004), whereas the effect of the membrane was approximated by the IMM1 implicit solvent model (Lazaridis et al., 2003) Standard parameters were used, modeling the solvent as water, and the interior of the membrane as cyclohexane.

The free energy of different interfacial arrangements was calculated using a Monte Carlo scheme. A step consisted in the choice of a putative new conformation obtained by rotating each receptor around the axis of its own helical bundle of a random angle (sampled from a uniform distribution $-30^\circ \leq \alpha, \beta \leq +30^\circ$), and increasing or decreasing the distance between the centers of mass of a random distance (-2 Å $\leq \delta \leq +2$ Å). Proposed moves were rejected if the distance between the centers of mass increased over 35 Å or if the distance between the two TM4 helices increased over 20 Å. A simulated annealing protocol was used to optimize the positions of the side chains of the putative conformations obtained after the proposed moves, keeping the TM Cα fixed. The total energy in the new conformation after the simulated annealing relaxation was used to either accept or reject the proposed move. The cycle was repeated 10^5 times, and the free energy was calculated as a function of the angles around the axis of the helix bundle of each protomer (α and β), integrating the dependence on the distance.

Metadynamics of the mGluR2/2AR Complexes Interacting at Symmetric TM4/TM4 or TM4,5/TM4,5 Interfaces

Based on the results of the conformational sampling of the ligand-free receptors and of the interface exploration, we built 4 different reference states for the symmetric TM4/TM4 interface of the clozapine-bound mGluR2/2AR complex, and 4 states for the symmetric TM4,5/TM4,5 interface of the methysergide-bound and the DOI-bound mGluR2/2AR complex, one for each conformation sampled along the activation pathway of mGluR2. These reference states were used to derive the path variables for three metadynamics simulations, a first one for the TM4/TM4 clozapine-bound mGluR2/2AR complex, a second one for the TM4,5/TM4,5 methysergide-bound mGluR2/2AR complex, and a third one for the TM4,5/TM4,5 DOI- bound mGluR2/2AR complex. We then reconstructed the free energy of activation of mGluR2 in the presence of the three different dimeric arrangements with clozapine-bound, the methysergide-bound and the DOI-bound 2AR. The parameters were the same as those used in the exploration of the 2AR conformational ensemble described above.

Analysis of mGluR2 and 2AR Protein Levels

Membrane fractions from oocytes expressing HA-tagged mGluR2, myc-tagged 2AR or both, were prepared as described previously (Michailidis et al., 2011). The pellets were resuspended with lysis buffer (0.5ml per oocyte), mixed with SDS-PAGE loading buffer, boiled for 10 min, and analyzed by western Blotting, using anti-HA (rat monoclonal anti-HA antibody 3F10; Boehringer Mannheim) and anti-myc (Myc-Tag 9B11 Mouse mAb, Cell Signaling Technology) antibodies. Protein levels for mGluR2 and 2AR were quantified by densitometric scanning and expressed relative to mGluR2 or 2AR levels in oocytes injected with 1 ng of mGluR2 + 2ng of 2AR mRNAs.

Measurement of Intracellular Ca^{2+}

For measurement of intracellular free calcium, mouse cortical primary cultures were plated in coverslips and incubated for 1 hr with 10 μM fura-2 (Molecular Probes Inc., USA). A photometry based epifluorescence microscopy system (Ionoptix; Milton, MA; objective, ×40; 0.9 numerical aperture) was used to detect the intracellular Ca^{2+} transient. A Hyperswitch (HSW400, Ionoptix; Milton, MA, USA) with a galvanometer driven mirror was used to alternatively excite fura-2 at wavelengths 340 and 380 nm at 2.5 Hz, and the Ca^{2+} transient was estimated as the ratio (f340/f380) of the emissions at 510 nm. Imaging was obtained using Ion Wizard fluorescence analysis software version 4.4. Experiments were performed on days 6, 7, and 8 after isolation. Image pairs were collected integrating a region of interest covering the whole cell at 2.5 Hz and filtered using a low-pass filter with a time constant $\tau = 1$ s to reduce noise. Intracellular calcium concentration $[Ca^{2+}]_i$ was expressed as a 340/380 nm ratio and its increase was normalized to the basal 340/380 nm ratio level before perfusion of the drug.

[^{3}H]Ketanserin and [^{35}S]GTPγS Binding Assays

Membrane preparations were incubated for 60 min at 37°C. Nonspecific binding was determined in the presence of 10 μM methysergide. [^{35}S]GTPγS binding experiments were initiated by the addition of membranes containing 35 μg of protein to an assay buffer (20 mM HEPES, 3 mM $MgCl_2$, 100 mM NaCl, 0.2 mM ascorbic acid and 0.5 nM [^{35}S]GTPγS) supplemented with 0.1 μM or 10 μM GDP for $G\alpha_{q/11}$ and $G\alpha_i$, respectively, and containing the indicated concentration of ligands. Nonspecific binding was determined in the presence of 100 μM GTPγS. Reactions were incubated for 30 min at 30°C, and were terminated by the addition of 0.5 ml of ice-cold buffer, containing 20 mM HEPES, 3 mM $MgCl_2$, 100 mM NaCl and 0.2 mM ascorbic acid. The samples were centrifuged at 16,000 g for 15 min at 4°C, and the resulting pellets were re-suspended in solubilization buffer (100 mM Tris, 200 mM NaCl, 1 mM EDTA, 1.25% Nonidet P40) plus 0.2% SDS. Samples were precleared with Pansorbin (Calbiochem), followed by immunoprecipitation with antibody against $G\alpha_{q/11}$or $G\alpha_{i1,2,3}$ (Santa Cruz Biotechnology). Finally, the immunocomplexes were washed twice with solubilization buffer, and bound [^{35}S]GTPγS was measured by liquid-scintillation spectrometry.

Coimmunoprecipitation in Mouse Frontal Cortex

Tissue samples of mouse frontal cortex were homogenized using a Teflon-glass grinder (10 up-and-down strokes at 1,500 rpm) in 1 ml of homogenization buffer (50 mM Tris-HCl, pH 7.4), supplemented with 0.25 M sucrose. The crude homogenate was centrifuged at 1,000 × g for 5 min at 4°C, and the supernatant was recentrifuged at 40,000 × g for 15 min at 4°C. The resultant pellet (P_2 fraction) was washed twice in homogenization buffer and recentrifuged in similar conditions. Aliquots of 1 mg of protein were stored at −80°C until coimmunoprecipitation assay. The protein pellets were resuspended in 1 ml RIPA buffer (150 mM NaCl, 5 mM EDTA, 0.8% SDS, 1% Triton X-100, 50 mM HEPES; pH 7.4, supplemented with protease inhibitors), and rotated at 4°C for 60 min. After centrifugation at 14,000 rpm for 15 min, 900 μl of the supernatant were rotated with 40 μl of protein A/G beads (Santa Cruz Biotechnology, Inc.) at 4°C for 60 min. After centrifugation at 14,000 rpm for 1 min, 400 μl of the supernatant were incubated overnight with 4 μl of anti-2AR antibody (Abcam, ab16028) and 40 μl of protein A/G beads at 4°C. Beads were then washed three times with RIPA buffer. Equal amounts of protein were resolved by SDS-polyacrylamide gel electrophoresis. Detection of proteins by immunoblotting using using anti-2AR and anti-mGluR2 (Abcam, ab15672) antibodies was conducted using the ECL system according to the manufacturer's instructions.

Cortical Primary Cultures and Immunocytochemistry

For cortical primary cultures, mice were sacrificed at the embryonic day (E) 15 stage. The media was removed and the cells were fixed with 3% formaldehyde in PBS for 15 min. The coverslips were washed with 3 × 2 ml PBS before being treated for 10 min with 0.3% Triton X-100 to permeabilize the cell membrane to antibodies. Coverslips were further washed with PBS and incubated in PBS containing 3% horse serum and 1% bovine serum albumin (blocking buffer) to reduce nonspecific binding. Primary antibodies anti-2AR and anti-mGluR2 (see above) were incubated for 60 min at room temperature. After washing with blocking buffer (3 × 2 ml), the cells were incubated with the secondary antibodies Alexa 488-conjugated goat anti-rabbit (Invitrogen, A11011) and Alexa 568-conjugated goat anti-mouse (Invitrogen, A11001) for 60 min at room temperature. After washing (PBS, 6 × 2 ml), the coverslips were dried and treated with antifade before being fixed onto glass slides.

For immunochemistry in brain section, mice were deeply anesthetized with with ketamine/xylazine. Transcardiac perfusion was performed with 10 ml PBS, followed by 30 ml of freshly prepared 4% paraformaldehyde (PFA) in PBS at room temperature. Brains were removed and immersion-fixed in 4% PFA in 1 ml at 4°C for 60 min and stored at 30% sucrose in PBS at 4°C for an additional 12 hr before to obtain the frontal cortex section. The slides were further washed with PBS and incubated in PBS containing 0.2% Tx-100 and 5% bovine serum albumin to permeabilize the cells. Primary antibodies anti-2AR and anti-mGluR2 (see above) were incubated for overnight at 4°C. After washing with PBS the slices were incubated with the secondary antibodies Alexa 488-conjugated goat anti-rabbit (Invitrogen, A11011) and Alexa 568-conjugated goat anti-mouse (Invitrogen, A11001) for 60 min at room temperature. After washing (PBS, 6 × 2 ml), the slices were mounted onto coverslips treated with antifade. Sections incubated with secondary antibody alone exhibited background immunofluorescence (data not shown). Tissue samples were examined by upright epifluorescence microscopy (Zeiss Axioplan 2IE).

SUPPLEMENTAL REFERENCES

Barducci, A., Bussi, G., and Parrinello, M. (2008). Well-tempered metadynamics: a smoothly converging and tunable free-energy method. Phys. Rev. Lett. *100*, 020603.

Bonomi, D., Branduardi, G., and Bussi, C. (2009). PLUMED: A portable plugin for free-energy calculations with molecular dynamics. Comput. Phys. Commun. *180*, 1961–1972.

Braden, M.R., Parrish, J.C., Naylor, J.C., and Nichols, D.E. (2006). Molecular interaction of serotonin 5-HT2A receptor residues Phe339(6.51) and Phe340(6.52) with superpotent N-benzyl phenethylamine agonists. Mol. Pharmacol. *70*, 1956–1964.

Branduardi, D., Gervasio, F.L., and Parrinello, M. (2007). From A to B in free energy space. J. Chem. Phys. *126*, 054103.

González-Maeso, J., Rodríguez-Puertas, R., and Meana, J.J. (2002). Quantitative stoichiometry of G-proteins activated by mu-opioid receptors in postmortem human brain. Eur. J. Pharmacol. *452*, 21–33.

Hof, P.R., et al (2000). Comparative Cytoarchitectonic Atlas of the C57BL/6 and 129/Sv Mouse Brains (Amsterdam: Elsevier).

Kanagarajadurai, K., Malini, M., Bhattacharya, A., Panicker, M.M., and Sowdhamini, R. (2009). Molecular modeling and docking studies of human 5-hydroxytryptamine 2A (5-HT2A) receptor for the identification of hotspots for ligand binding. Mol. Biosyst. *5*, 1877–1888.

Lazaridis, T. (2003). Effective energy function for proteins in lipid membranes. Proteins *52*, 176–192.

MacKerell, A.D., Bashford, D., and Bellot, M. (1998). All-atom empirical potential for molecular modeling and dynamics. J. Phys. Chem. *102*, 3586–3616.

Mackerell, A.D., Jr., Feig, M., and Brooks, C.L., 3rd. (2004). Extending the treatment of backbone energetics in protein force fields: limitations of gas-phase quantum mechanics in reproducing protein conformational distributions in molecular dynamics simulations. J. Comput. Chem. *25*, 1400–1415.

Michailidis, I.E., Rusinova, R., Georgakopoulos, A., Chen, Y., Iyengar, R., Robakis, N.K., Logothetis, D.E., and Baki, L. (2011). Phosphatidylinositol-4,5-bisphosphate regulates epidermal growth factor receptor activation. Pflugers Arch. *461*, 387–397.

Morris, B.J., Cochran, S.M., and Pratt, J.A. (2005). PCP: from pharmacology to modelling schizophrenia. Curr. Opin. Pharmacol. *5*, 101–106.

Phillips, J.C., Braun, R., Wang, W., Gumbart, J., Tajkhorshid, E., Villa, E., Chipot, C., Skeel, R.D., Kalé, L., and Schulten, K. (2005). Scalable molecular dynamics with NAMD. J. Comput. Chem. *26*, 1781–1802.

Rasmussen, S.G., DeVree, B.T., Zou, Y., Kruse, A.C., Chung, K.Y., Kobilka, T.S., Thian, F.S., Chae, P.S., Pardon, E., Calinski, D., et al. (2011). Crystal structure of the β2 adrenergic receptor-Gs protein complex. Nature *477*, 549–555.

Roth, B.L., Shoham, M., Choudhary, M.S., and Khan, N. (1997). Identification of conserved aromatic residues essential for agonist binding and second messenger production at 5-hydroxytryptamine2A receptors. Mol. Pharmacol. *52*, 259–266.

Scheerer, P., Park, J.H., Hildebrand, P.W., Kim, Y.J., Krauss, N., Choe, H.W., Hofmann, K.P., and Ernst, O.P. (2008). Crystal structure of opsin in its G-protein-interacting conformation. Nature *455*, 497–502.

Vanommeslaeghe, K., Hatcher, E., Acharya, C., Kundu, S., Zhong, S., Shim, J., Darian, E., Guvench, O., Lopes, P., Vorobyov, I., and Mackerell, A.D., Jr. (2010). CHARMM general force field: A force field for drug-like molecules compatible with the CHARMM all-atom additive biological force fields. J. Comput. Chem. *31*, 671–690.

Vivaudou, M., Chan, K.W., Sui, J.L., Jan, L.Y., Reuveny, E., and Logothetis, D.E. (1997). Probing the G-protein regulation of GIRK1 and GIRK4, the two subunits of the KACh channel, using functional homomeric mutants. J. Biol. Chem. *272*, 31553–31560.

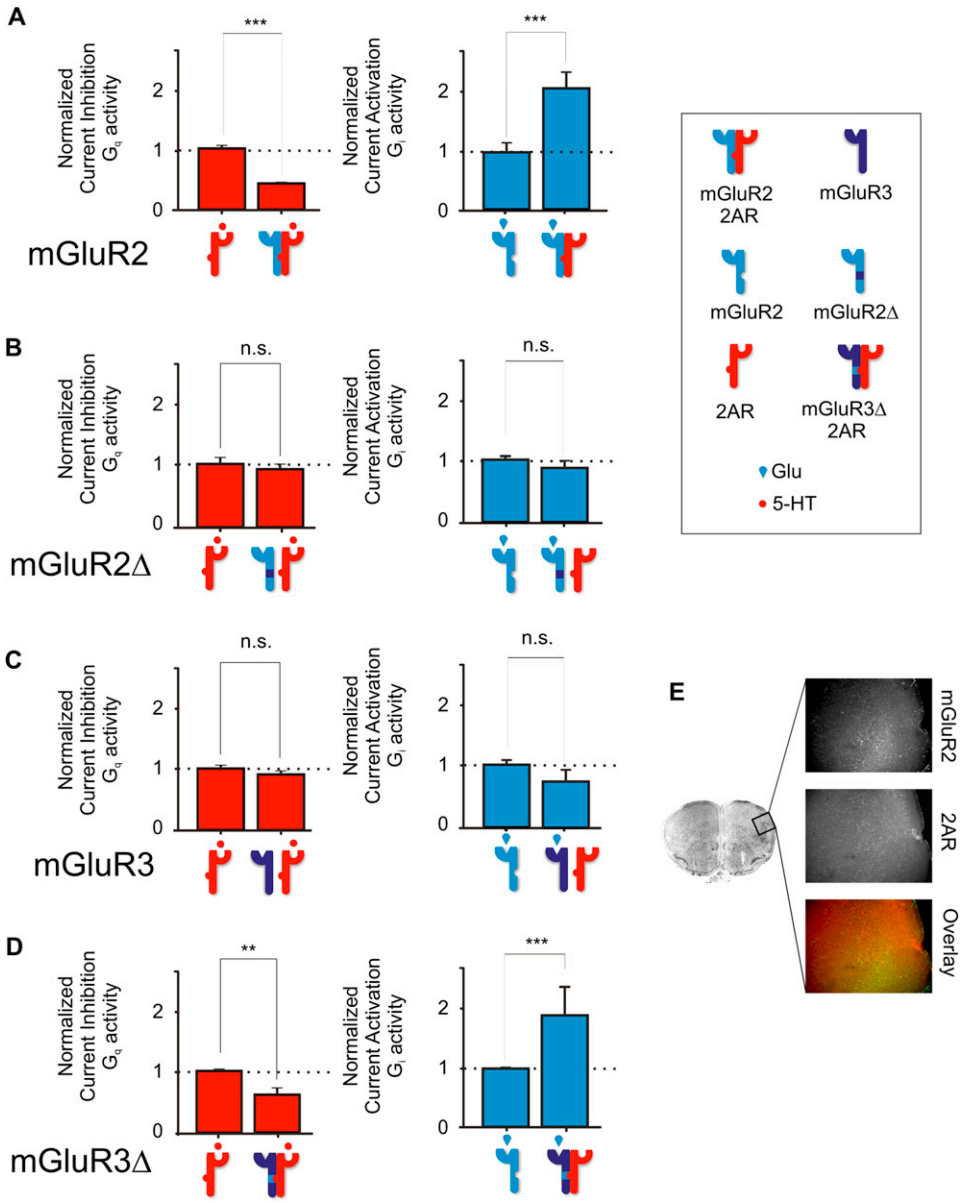

Figure S1. The Increase in Gi Signaling and Decrease in Gq Signaling Depend on Heterocomplex Formation, Related to Figure 1

Bar graph summary of IRK3 current inhibition (left) and GIRK4* current activation (right) (mean ± SEM) in oocytes expressing 2AR alone or 2AR together with mGluR2 (A), mGluR2Δ (B), mGluR3 (C), or mGluR3Δ (D). IRK3 current inhibition and GIRK4* current activation were measured and normalized as in Figures 1D and 1E, respectively. Currents were obtained in response to 1 μM of the endogenous ligand serotonin (5-HT) and 1 μM of endogenous ligand glutamate (Glu). Coexpression of mGluR2Δ with 2AR did not result in a significant decrease in Gq signaling in response to 5-HT or a significant increase in Gi signaling in response to Glu (C) when compared to the group coexpressing mGluR2 and 2AR (A). Similarly, both effects were absent for mGluR3 (B), but present for mGluR3Δ (D) (**$p < 0.01$; ***$p < 0.001$; n.s., not significant). The Nissl staining of the coronal cortex was taken from the mouse brain atlas with the author's permission (Hof et al., 2000). (E) Representative epifluorescence micrographs showing coexpression of endogenous 2AR (red) and mGluR2 (green) in mouse frontal cortex sections. Scale bar, 100 μm.

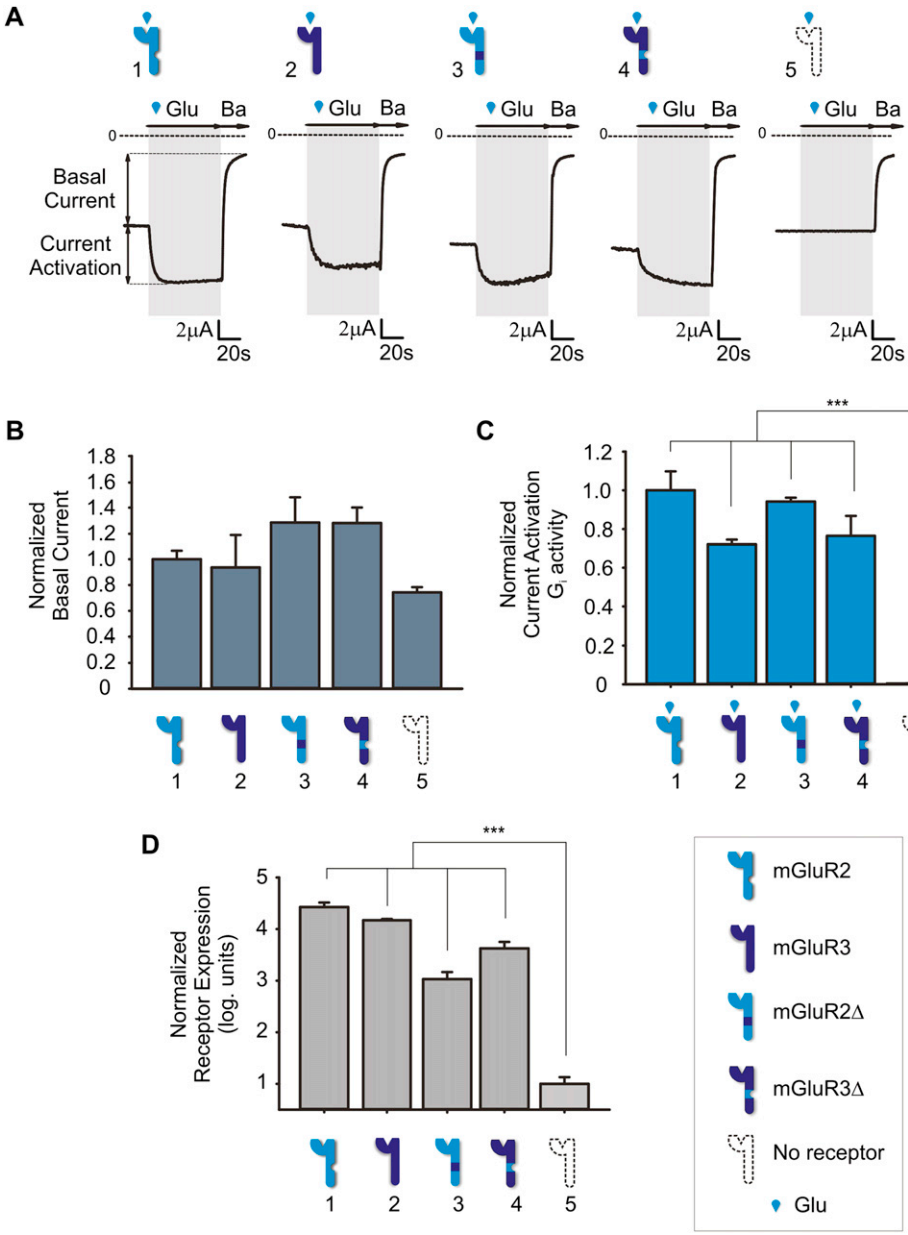

Figure S2. Expression Levels of mGluR2, mGluR2Δ, mGluR3, and mGluR3Δ, Related to Figure 1

(A) Representative GIRK4* barium-sensitive traces obtained in response to 1 μM glutamate. mGluR2, mGluR2Δ, mGluR3Δ, and mGluR3Δ were functional as Gi-coupled GPCRs.

(B) Statistical summary of basal current (mean ± SEM) (***$p < 0.001$).

(C) Statistical summary of glutamate agonist-induced current (mean ± SEM). GIRK4* current activation was measured and normalized as in Figure 1D. Current activation for mGluR2 (1), mGluR3 (2), mGluR2Δ (3), and mGluR3Δ (4) were similar compared with noninjected (5) (***$p < 0.001$).

(D) Data summary (mean ± SEM) of measured receptor membrane expression levels. Expression was measured with surface labeled receptors and quantitated with a chemiluminescence assay. Chemiluminescence intensity is expressed in logarithmic units and normalized to the background noninjected intensity level. Expression levels were similar for all constructs (1, 2, 3, and 4) compared to noninjected (5) (***$p < 0.001$; n.s, not significant).

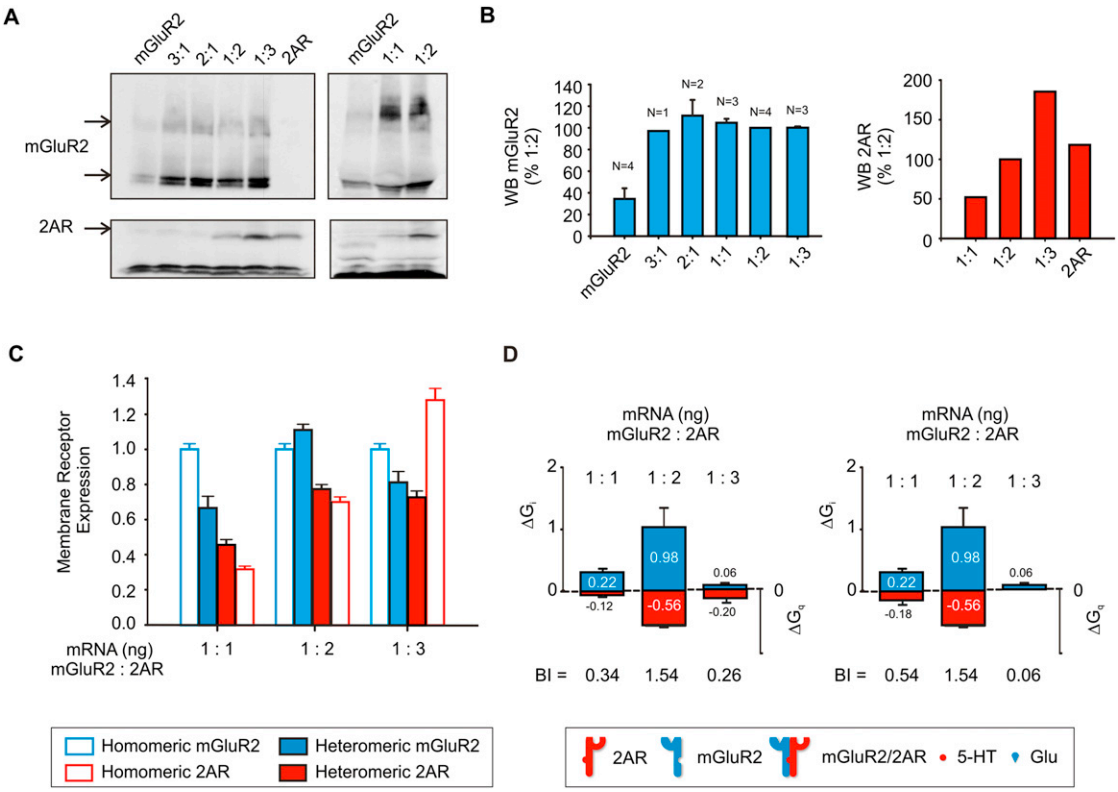

Figure S3. Changes in Injected 2AR mRNA Alter Expression Levels of the Complex in the Membrane and the Difference in Gi to Gq Signaling, Related to Figure 1

(A) Western blot analysis of the membrane fraction of oocytes, injected with 1 ng of HA-tagged mGluR2 RNA (mGluR2), or 2 ng of myc-tagged 2AR RNA (2AR), or 1 ng of HA-tagged mGluR2 RNA plus various amounts of 2AR RNA (mGluR2/2AR RNA ratios are shown on top of each lane).

(B) Summary of densitometry data for mGluR2 (left) and 2AR (right) from experiments such as the one shown in (A), normalized relative to mGluR2 (left) or 2AR (right) protein levels in oocytes injected with 1 ng of mGluR2 + 2 ng of 2AR mRNAs. Data are from 1–4 independent experiment (see numbers on top of each bar). "mGluR2" indicates homomeric expression of 1 ng mGluR2 mRNA and "2AR" indicates homomeric expression of 2 ng of 2AR mRNA.

(C) Expression levels of mGluR2 (blue filled bars) and 2AR (red filled bars) in the membrane. Data summary (mean ± SEM) of measured receptor membrane expression levels (as were shown in Figure S2D) for oocytes injected with 1 ng of mGluR2 mRNA and 1 ng, 2 ng, and 3 ng of 2AR mRNA, respectively. Expression was measured with surface-labeled receptors and quantitated with a chemiluminescence assay. Chemiluminescence was normalized to the signal obtained in oocytes injected with 1 ng of mGluR2 alone (empty blue bars). For reference, the levels corresponding to oocytes injected with 1 ng, 2 ng, and 3 ng of 2AR alone are also depicted (empty red bars). All signal levels were at least 500 times higher than background.

(D) Changes in injected 2AR mRNA alter the Gi and Gq balance. ΔGi and ΔGq measured in oocytes injected with 1 ng mGluR2 mRNA and 1 ng, 2 ng, and 3 ng of 2AR mRNA, respectively. ΔGi is referenced to the homomeric mGluR2 (1 ng or mRNA) response to 1 μM glutamate. (Left) ΔGq is referenced to multiple homomeric 2AR responses to 1 μM serotonin corresponding to 1 ng, 2 ng, and 3 ng of injected 2AR mRNA. (Right) ΔGq is referenced to one single homomeric response to 1 μM serotonin corresponding to 2 ng injected 2AR mRNA. Data are mean ± SEM.

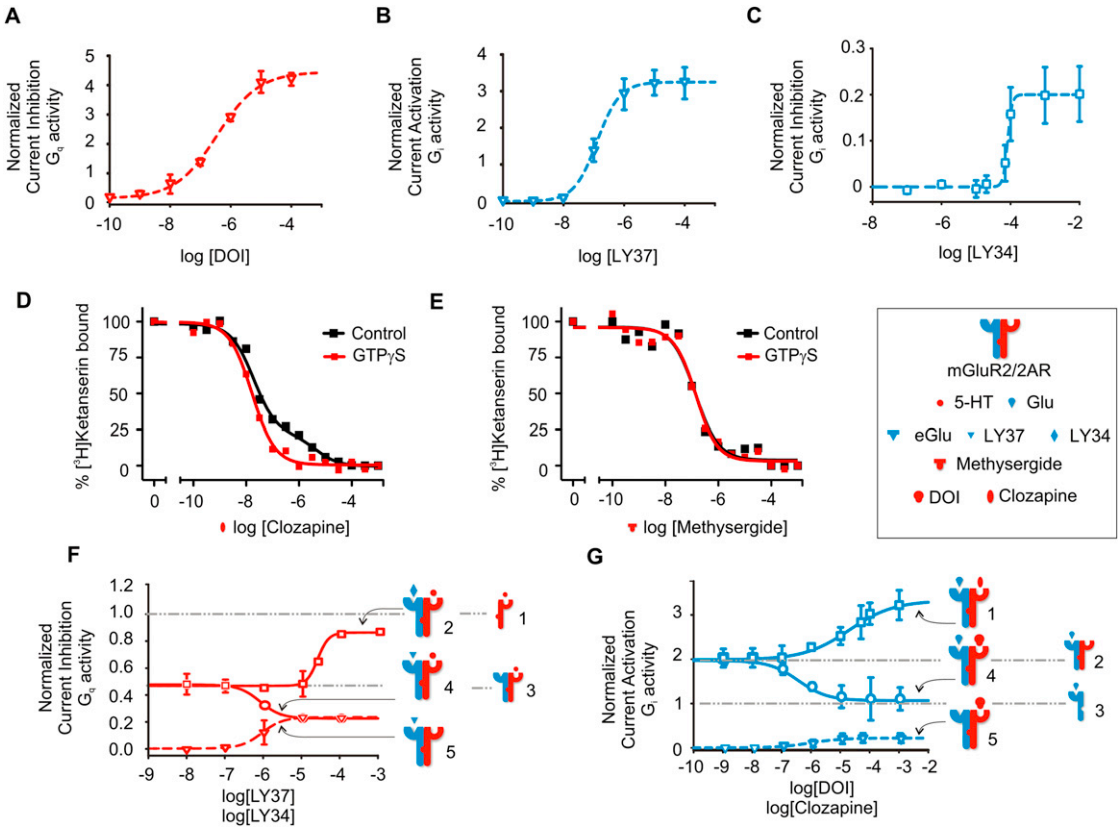

Figure S4. Homomeric and Heteromeric Dose-Response Curves for DOI, LY37, and LY34, Related to Figure 3

(A) Dose-response curve showing normalized Gq activation elicited by DOI in oocytes expressing 2AR. Gq-mediated IRK3 current inhibition was measured and normalized as in Figure 1D ($EC_{50} = 3.6 \times 10^{-7} \pm 1.05 \times 10^{-7}$).

(B) Dose-response curve showing normalized Gi activation elicited by LY37 in oocytes expressing mGluR2. Gi-mediated GIRK4* current stimulation was measured and normalized as in Figure 1E ($EC_{50} = 1.3 \times 10^{-7} \pm 6.4 \times 10^{-9}$).

(C) LY34 behaves as an inverse agonist. Dose-response curve showing normalized Gi inhibition elicited by LY34 in oocytes expressing mGluR2. Gi-mediated GIRK4* current inhibition was measured and normalized as in Figure 1E. Gi inhibition is shown indicating LY34 inverse agonism ($IC_{50} = 8.2 \times 10^{-5} \pm 1.7 \times 10^{-6}$).

(D and E) Clozapine, and not methysergide, behaves as an inverse agonist in mouse frontal cortex membrane preparations. [^{3}H]Ketanserin binding displacement curves by clozapine (D) or methysergide (E) in the absence (black) and in the presence (red) of 10 μM GTPγS. Clozapine displacing [^{3}H]ketanserin binding: $pK_{i\text{-high}}$ control, −8.01 ± 0.1; $pK_{i\text{-low}}$ control, −5.64 ± 0.4; fraction high, 0.77 ± 0.06; pK_i GTPγS, −8.07 ± 0.05 (F [3,78] = 4.99, $p < 0.01$). Methysergide displacing [^{3}H]ketanserin binding: pK_i control, −7.16 ± 0.08; pK_i GTPγS, −7.15 ± 0.07 (F [3,88] = 0.05, $p = 0.98$).

(F) Dose-response curves showing cross signaling with LY37 in the absence of serotonin (5) ($EC_{50} = 9.34 \times 10^{-7} \pm 1.13 \times 10^{-7}$), dominant-agonist effect with LY37 (4) ($EC_{50} = 8.35 \times 10^{-7} \pm 3.37 \times 10^{-8}$), and inverse-agonist effect with LY34 (2) ($EC_{50} = 8.2 \times 10^{-5} \pm 1.6 \times 10^{-6}$) and serotonin signaling. The Gq response by heteromer formation is indicated by the dashed lines [from (1) to (3)] (see also Figures S6A and S6B for LY37 effects in 2AR-KO mice).

(G) Dose-response curves showing cross signaling with DOI in the absence of glutamate (5) ($EC_{50} = 9.49 \times 10^{-7} \pm 4.3 \times 10^{-7}$), dominant-agonist effect with DOI (4) ($EC_{50} = 3.72 \times 10^{-7} \pm 8.45 \times 10^{-8}$), and inverse-agonist effect with clozapine (1) ($EC_{50} = 2.02 \times 10^{--5} \pm 7.10 \times 10^{-6}$) of Glu signaling. The Gi response by heteromer formation is indicated by the dashed lines [from (3) to (2)].

Data are mean ± SEM.

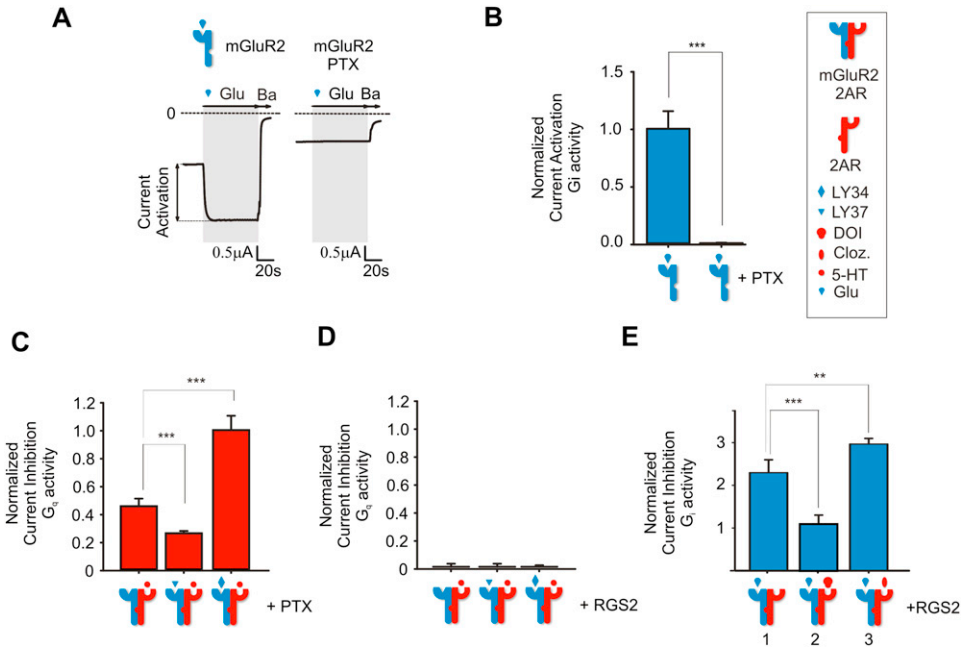

Figure S5. LY37 and LY34 Effects on Gq Activity Are PTX Insensitive but RGS Sensitive, Related to Figure 3

(A) Representative GIRK4* barium-sensitive current traces in oocytes expressing mGluR2 alone or mGluR2 together with PTX.

(B) Bar graph summary of normalized Gi activity (mean ± SEM) elicited by glutamate (1 μM) in the presence and absence of PTX. GIRK4* current activation was measured and normalized as in Figure 1E.

(C and D) Bar graph summary of Gq activity (mean ± SEM) in response to 5-HT (1 μM) alone, or together with LY37 (10 μM) or LY34 (10 μM), measured in oocytes expressing mGluR2, 2AR, and PTX (C) or RGS2 (D). IRK3 current inhibition was measured and normalized as in Figure 1D.

(E) Bar graph summary of Gi activity (mean ± SEM) measured in oocytes expressing mGluR2, 2AR, and RGS2. GIRK4* current activation was measured and normalized as in Figure 1E.

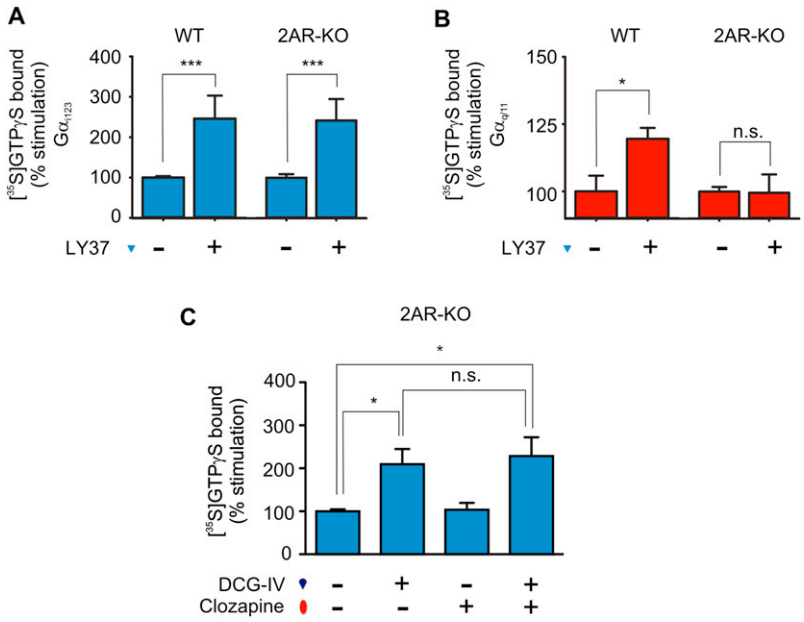

Figure S6. Biochemical Studies in 2AR-KO Mouse Frontal Cortex: LY37-Mediated Gi Activation Is Unaffected, whereas Gq Activation and Upmodulation of mGluR2-Dependent Gi Signaling by Clozapine Are Abolished, Related to Figure 5

(A and B) LY37-stimulated [^{35}S]GTPγS binding in wild-type (WT) and 2AR-KO mouse frontal cortex membrane preparations followed by immunoprecipitation with anti-Gαi (A) or anti-Gαq (B) antibodies after treatment with vehicle or 10 μM LY37. Data are mean ± SEM (*$p < 0.05$; ***$p < 0.001$; n.s., not significant).

(C) DCG IV-stimulated [^{35}S]GTPγS binding in 2A-KO mouse frontal cortex membranes followed by immunoprecipitation with anti-Gαi antibody in the presence or clozapine or vehicle. Data are mean ± SEM (*$p < 0.05$; n.s., not significant). (Compare with Figure 5A in wild-type mice.)

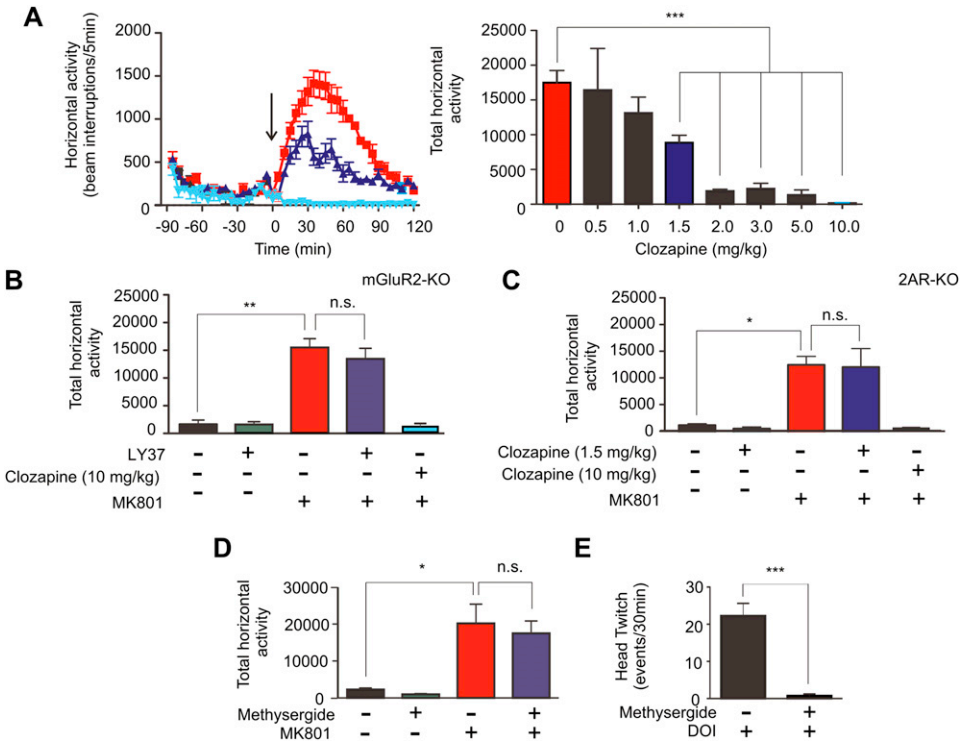

Figure S7. Dose-Response Effect of Clozapine in the Locomotor Response Induced by MK801, Related to Figure 5

(A) Left panel depicts representative time courses of MK801-induced locomotion measured in 5 min block. Mice were administered clozapine (1.5 or 10 mg/kg) or vehicle followed by MK801 (0.5 mg/kg). Time of injection is indicated by arrow. The right panel shows bar graph summaries of the total of MK801-induced locomotion as a summation of horizontal activity from t = 30 min to t = 120 min. Mice were administered clozapine (at the indicated dose) or vehicle followed by MK801 (0.5 mg/kg). Data are mean ± SEM (n = 5-20); (*$p < 0.05$; **$p < 0.01$; n.s., not significant).

(B and C) Data summary of the total MK801-induced locomotion as a summation of horizontal activity from t = 30 min to t = 120 min. mGluR2-KO (B) and 2AR-KO mice (C) were administered clozapine at 10 mg/kg (cyan), and we compared the response to that of LY37 (purple), or clozapine at 1.5 mg/kg (purple), or vehicle (red), followed by MK801. Data are mean ± SEM (n = 4–10); (*$p < 0.05$; **$p < 0.01$; n.s., not significant).

(D and E) Methysergide does not modulate the locomotor response induced by MK801 but abolishes the head-twitch response induced by DOI. (D) Mice were administered methysergide (3 mg/kg) or vehicle, followed by MK801 (0.5 mg/kg) or vehicle. Data are mean ± SEM (n = 4–6) (*$p < 0.05$; n.s., not significant). (E) Head-twitch response was determined in mice injected with DOI (2 mg/kg) 15 min after being injected with methysergide (3 mg/kg). Data are mean ± SEM (n = 5 per group). ***$p < 0.001$. These data suggest that although methysergide binds as a neutral antagonist to 2AR and blocks the behavioral responses induced by 2AR agonists, it does not induce antipsychotic-like effects.

Gi	mGluR2 / 2AR	mGluR2Δ / 2AR	mGluR3 / 2AR	mGluR3Δ / 2AR
5-HT	0.43 ± 0.04	1.02 ± 0.23	0.98 ± 0.14	0.65 ± 0.26
5-HT + LY34	0.83 ± 0.18	1.07 ± 0.17	0.98 ± 0.16	1.00 ± 0.13
5-HT + LY37	0.23 ± 0.03	1.00 ± 0.05	0.87 ± 0.31	0.23 ± 0.14
LY37	0.26 ± 0.14	0.02 ± 0.01	0.021 ± 0.01	0.11 ± 0.06
Gq	**mGluR2 / 2AR**	**mGluR2Δ / 2AR**	**mGluR3 / 2AR**	**mGluR3Δ / 2AR**
Glu	1.98 ± 0.87	0.94 ± 0.27	1.07 ± 0.17	2.30 ± 0.68
Glu + Clozapine	2.80 ± 0.37	1.23 ± 0.32	0.90 ± 0.11	2.97 ± 0.29
Glu + DOI	0.99 ± 0.22	1.23 ± 0.24	1.07 ± 0.32	1.12 ± 0.37
DOI	0.35 ± 0.18	0.01 ± 0.00	0.01 ± 0.00	0.37 ± 0.16

Table S1. Cross-Signaling, DownModulation, and Upmodulation Depend on Heterocomplex Formation, Related to Figure 2

Summary of GIRK4* current activation (Gi) and IRK3 current inhibition (Gq) (mean ± SD) in oocytes expressing 2AR alone or 2AR together with mGluR2, mGluR2Δ, mGluR3, or mGluR3Δ. IRK3 current inhibition and GIRK4* current activation were measured and normalized as in Figure 1, D and E respectively. Currents were obtained in response to 1 μM of the endogenous ligand serotonin (5-HT) and 1 μM of endogenous ligand glutamate (Glu). For Gq values were obtained in response to 1 μM of the endogenous ligand serotonin (5-HT), 1 μM serotonin together with 50 μM LY34, serotonin 1 μM together with 50 μM LY37, or 50 μM LY37 alone. For Gi values were obtained in response to 1 μM of the endogenous ligand glutamate (Glut), 1 μM glutamate together with 50 μM clozapine, serotonin 1 μM together with 50 μM DOI, or 50 μM DOI alone. Gq: 5-HT, 5-HT + LY34, and 5-HT + LY37 treatments were significantly different for mGluR2/2AR and mGluR3Δ/2AR ($p<0.05$). Gi: Glu, Glu + Clozapine, and Glu + DOI treatments were only significantly diffferent for mGluR2/2AR and mGluR3Δ/2AR ($p<0.005$).

	Δ Gi	Δ Gq	BI_{10}	Δ Gi	Δ Gq	BI_{50}
Clozapine	1.32	-0.98	**2.3**	1.68	-0.98	**2.66**
Risperidone	1.36	-0.82	**2.18**	1.69	-0.9	**2.59**
LY37	1.45	-0.65	**2.1**	1.55	-0.77	**2.32**
Ritanserin	1.12	-0.77	**1.89**	1.17	-0.85	**2.02**
Methysergide	0.96	-0.80	**1.76**	0.95	-0.82	**1.77**
eGlu	0.54	-0.44	**0.98**	0.39	-0.45	**0.84**
LY34	-1.02	-0.20	**-0.82**	-1.07	-0.17	**-0.9**
DOI	-0.01	0.95	**-0.96**	-0.01	1.39	**-1.4**

Table S2. Balance Index Calculations, Related to Figure 4

Balance Index (BI) Calculations for clozapine, risperidone, LY37, methysergide, eGlu, LY34 and DOI at 10 μM (BI_{10}) and 50 μM concentration (BI_{50}).